Interaction of Water Highly Diluted in 1-Alkyl-3-methyl Imidazolium Ionic Liquids with the PF_6^- and BF_4^- Anions

Y. Danten,*,† M. I. Cabaço,‡ and M. Besnard†

Institut des Sciences Moléculaires, CNRS (UMR 5255), Université Bordeaux, 351, Cours de la Libération 33405 Talence Cedex, France, and Centro de Física Atómica da UL, Av. Prof. Gama Pinto 2, 1694-003 Lisboa Codex and Departamento de Física, Instituto Superior Técnico, UTL, Av. Rovisco Pais 1049-001 Lisboa, Portugal

Received: December 9, 2008; Revised Manuscript Received: January 9, 2009

We have investigated water highly diluted in 1-alkyl-3-methyl imidazolium ionic liquids (ILs) with hexafluorophosphate $\{PF_6^-\}$ and tetrafluoroborate $\{BF_4^-\}$ anions using vibrational spectroscopic measurements in the ν_{OH} spectral domain of water (3600−3800 cm^{-1}) and DFT calculations. The measured profiles exhibit two well-defined bands at coinciding vibrational transitions assigned with the ν_1 symmetric and ν_3 antisymmetric OH stretching modes of monodispersed water. The local organization and the vibrational spectra of water diluted in ILs have been assessed by DFT calculations (using the B3LYP functional and 6-31+G** basis set). We show that the predicted structures of water interacting (minimally) with two anions in nearly "symmetric" structures of type (A···H−O−H···A) lead to spectral features consistent with the previous spectroscopic observations as well as with those reported here. We emphasize the role of the non additive interaction forces (especially the 3-bodies electrostatic interactions) in the structural organization taking place between the cation−anion couples and for determining preferentially (A···H−O−H···A) associations of water with the anions as well as their consequences on the vibrational spectra of water. We show that the doubly hydrogen-bonded character of water in such associations leads to well-defined spectral features, which are the shifts of the ν_1 and ν_3 stretching modes of water, the separation $\Delta\nu_{13}$ between them (about 80 cm^{-1}), and the intensity ratio estimates $R = I\nu_3/I\nu_1$ (IR absorption and Raman). Finally, we evoke the fact that the H-bond interactions of water diluted in these ILs involve a more noticeable electrostatic character than for H-bond interactions of water in usual molecular solvents. In this context, we emphasize that the appearance of the Raman band of the ν_3 mode of water originates from a significant polarization of water due to the local electrostatic fields induced by surrounding ions.

I. Introduction

Ionic liquids (ILs) constitute a novel class of suitable environmental friendly ("green") solvents presenting an interesting alternative to traditional solvents in many applications such as organic/inorganic synthesis, catalysis, separations, and electro-chemistry[1−4] and provide new paths for chemical reactions and industrial applications due to their remarkable physical-chemical properties.[5−10] Comparatively with conventional organic solvents, they offer real advantages, which are mainly related to their specific properties such as a very low vapor pressure (making them environmentally compatible), a large liquidus range (at room temperature) associated with a significant polarity, high thermal conductivity, and wide electrochemical windows.[5,8,9,11−21] Non aqueous ionic liquids are typically composed of organic cations with organic or inorganic anions and are able to solubilize a broad variety of polar and nonpolar molecules, organic and inorganic materials (salts, proteins, amino acids, polysaccharides, etc.), as well as organometallic compounds. Interestingly, these properties are easily tuned by substituting the cation and/or the anion of the anion−cation couple. For instance, it has been recently shown that the density of ILs increases with a decrease of the alkyl chain length of the cation, leading to an apparent increase of the molecular weight of the anion.[4] In the same way, by changing the anion of the anion−cation couple, the liquid phase properties of ILs (density, viscosity, etc.) and especially its miscibility with respect to usual organic compounds (such as alcohols and water) can be drastically modified.[8,15,16,18,22]

In this context, it appeared of importance to carefully control the purity of the ionic liquids used for engineering applications, in particular, the presence of impurities as they can drastically alter their properties (density, viscosity, polarity, and conductivity) even at very small concentrations.[5,7,8,16−18,23] From this point of view, the presence of water can drastically change the solvent properties of 1-alkyl-3-methyl imidazolium-based ILs, which are hygroscopic and can absorb a significant amount of water from the atmosphere affecting the solubility estimation of diluted organic, inorganic, or gaseous substances. Moreover, small amounts of water can drastically modify the rates and selectivity of chemical reactions (reactants) in ILs.[7,8]

The study of the interactions between water and ILs has been also addressed from a fundamental point of view.[12,13,24−36] Recently, molecular dynamics simulation studies reveal that in the presence of water, 1-alkyl-3-methyl imidazolium-based ILs exhibit nanoscale structural organization with polar and nonpolar regions.[37−40] As the water concentration increases, the polar (ionic) network increasingly collapses at the expense of the formation of small water aggregates, which in turn leads to the

* Corresponding author. E-mail: y.danten@ism.u-bordeaux1.fr.
† Université Bordeaux.
‡ Instituto Superior Técnico.

10.1021/jp8108368 CCC: $40.75
Published on Web 03/03/2009

formation of a well-defined water hydrogen-bonds network at high water content.[39,41]

Interactions and molecular states of water have been also experimentally investigated using vibrational spectroscopy.[42−47] Indeed, it is established that infrared (IR) absorption spectroscopy is well-adapted for providing insight into the nature of the water interactions with its close environment especially through the OH-stretching modes of water situated in the 3000−3800 cm^{-1} spectral range. In particular, these modes are very sensitive to hydrogen-bond interactions of water molecules with a large variety of chemical species as surrounding solvent medium, including ILs. From the observed IR spectral features, it was concluded that at low water content in ILs, monomeric water molecules (i.e., non self-associated with itself) are present and mostly form symmetrical 1:2 H-bonded type complexes with two separate anions.[47] Recent dielectric spectroscopic measurements came to a similar conclusion about the molecularly dispersed presence of water in 1-alkyl-3-methyl imidazolium-based ILs mixtures at a molar fraction of water lower than 0.2.[41]

These findings agree nicely with the fact that the solubility of water in ILs (or the degree of hydroscopic character) strongly depends on the nature of the anion. For instance, the amount of water absorbed in 1-alkyl-3-methyl imidazolium-based ILs is found higher with BF_4^- than with PF_6^- anions.[5,45] In other terms, the solubility of water is closely related to the water−anion interaction strength in such a way that it has been possible to build a hydrophilic scale for ILs similarly to that established for solutions of water highly diluted in hydrophobic solvents in liquid phase[48−51] (and references therein) and in supercritical conditions.[50,52−59]

The present Article is aimed at investigating the detailed nature of interactions of water highly diluted in 1-alkyl-3-methyl imidazolium-based ILs with BF_4^- and PF_6^- anions. In this study, our methodology is based on an approach combining vibrational spectroscopy (IR absorption and Raman scattering) and DFT calculations to assess the nature of the local organization of diluted water in these imidazolium-based ILs. For this purpose, we present the analysis of the measured IR absorption and Raman spectra of water diluted in 1-methyl,3-butyl imidazolium (labeled as C_{4Mim}^+ or B_{Mim}^+) B_{Mim}^+/PF_6^- and B_{Mim}^+/BF_4^- solutions, focusing in the spectral region of the OH stretching modes (section II).

These experimental results will be interpreted and rationalized in the light of a theoretical investigation based upon DFT calculations (section III). One of the issues addressed in this work will concern the fundamental role of the many-body interactions in the BF_4^- and PF_6^-/imidazolium-based ILs by determining the local structure of water and their influence on the main spectral signatures. These discussions mainly concern the spectral features associated with the internal modes of water as well as the vibrational modes of the different ionic species, the imidazolium ring CH stretches and the BF and PF stretches of the BF_4^- and PF_6^- anions, respectively. These findings will be discussed in depth by underlying the close relationship existing between these spectral features and the nature of the water interactions in hydrophobic (with PF_6^-) and hydrophilic (with BF_4^-) imidazolium-based ionic solvents (section IV).

II. Experimental Spectra of Water in ILs

We have selected in our experiments two ILs involving the hexafluorophosphate {PF_6^-} (I) and the tetrafluoroborate {BF_4^-} (II) anions and having B_{Mim}^+ as cation (originating from Solvionic Co., with Cl, Br, I < 5 ppm). Because we are mostly interested in studying qualitatively monomeric water to understand its interactions with the ions forming the ILs, we have restricted our study to mixtures having a very low content of water resulting from absorbed atmospheric water. We have measured the amount of water, which is 0.5 M (0.09 m.f.) and 0.1 M (0.02 m.f.) in $B_{Mim}BF_4^-$ and $B_{Mim}PF_6^-$, respectively. For $B_{Mim}PF_6^-$, the water amount is smaller than the solubility reported in the literature.[5,16,45]

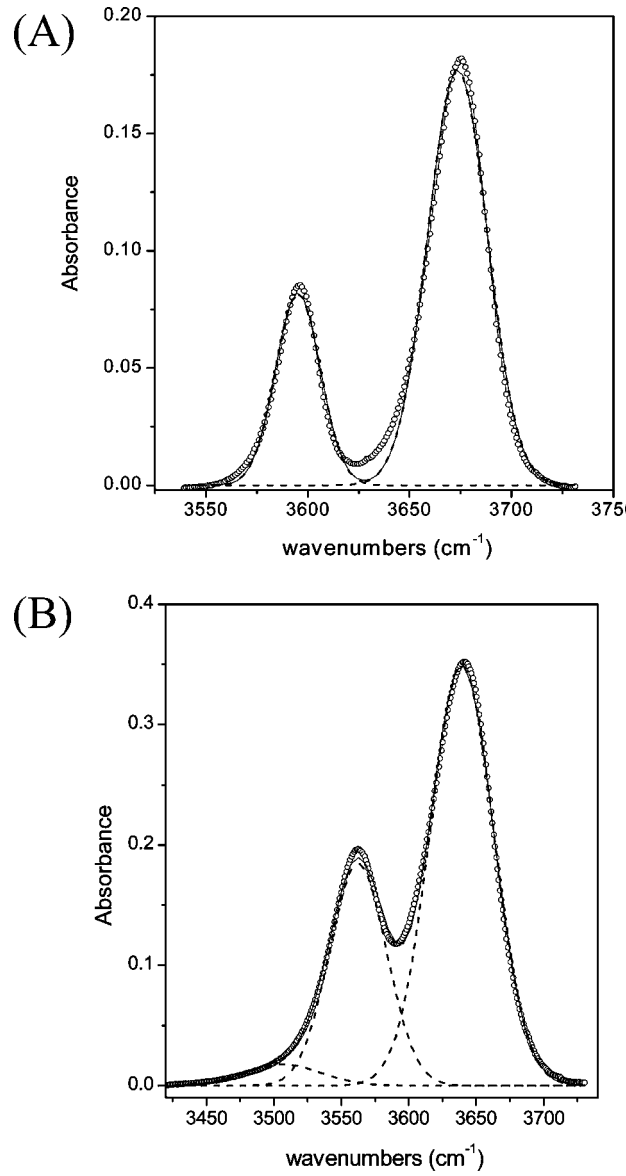

Figure 1. Measured (○) IR absorption spectra of water in the OH stretching modes region (3500−3800 cm^{-1}) in the PF_6/B_{Mim} (A) and BF_4/B_{Mim} (B) mixtures (water content about 1% in volume). Fitted Gaussian profiles (- - -) are also reported.

The infrared spectra have been measured on a Biorad Fourier transform interferometer equipped with a DTGS detector and a Ge/KBr beam splitter and have been obtained at 2 cm^{-1} spectral resolution after averaging of 50 scans. The Raman spectra have been measured on a Dilor confocal spectrometer equipped with a 1800 lines/mm grating (3 cm^{-1} spectral resolution) and a CCD detector using the 514.5 nm excitation line of an Ar^+ laser at a power of 20 mW. Spectra were recorded without polarization analysis with a typical acquisition time of about 120 s.

II.1. Infrared Spectra. The measured infrared spectra of these systems in the ν_{OH} spectral region are reported in Figure 1. At a glance, it appears that all of these spectra are mostly composed of two intense broad bands, which can be assigned

TABLE 1: Band-Shape Parameters of the Fitted Curves Obtained from the Measured Absorption Infrared and Raman Scattering Profiles Associated with the Internal Modes of Water in Imidazolium Ionic Liquids (under Atmospheric Moisture)[a]

		ν_1 mode of water		ν_3 mode of water		IR absorption
		IR	Raman	IR	Raman	$\nu_2 + \nu_3$ band
$B_{Mim}-PF_6^-$	band center (cm^{-1})	3595	3600	3674	3677	5277
	fwhh (cm^{-1})	19	20	28	30	28
	$R = I\nu3/I\nu1$	3.4	0.15			
$B_{Mim}-BF_4^-$	band center (cm^{-1})	3562	3565	3640	3643	5257
	fwhh (cm^{-1})	47	39	46	41	43−49
	$R = I\nu3/I\nu1$	1.9	0.18			

[a] The fitted profiles are Lorentzian in Raman absorption and Gaussian in infrared absorption.

to the ν_1 symmetric and ν_3 antisymmetric OH stretching vibrations of nonself-aggregated water (so-called "monomeric" water). In the B_{Mim}^+/BF_4^- mixture (II), we notice also a broad very weak low wavenumbers feature centered at about 3500 cm^{-1} (Figure 1B), which might reveal the presence of small water aggregates. In contrast, this band is not detected in the B_{Mim}^+/PF_6^- mixture (I) as expected for this hydrophobic ionic liquid.

These spectra have been found to be nicely fitted by Gaussian profiles (Figure 1), and the parameters deduced from these fits are collected in Table 1. We have also succeeded in measuring for the two systems the $\nu_3 + \nu_2$ combination band (where ν_2 is the water bending mode). The band shape corresponding to this transition was found to be almost Gaussian (Figure 2), and the corresponding fitted parameters are also reported in Table 1.

II.2. Raman Spectra. The Raman spectra measured in the OH stretching region are displayed for systems (I) and (II) in Figure 3. The spectra are composed of an intense profile observed in the spectral range 3560−3600 cm^{-1} accompanied on its high wavenumbers flank by a much weaker profile approximately centered in the range 3640−3670 cm^{-1}. Clearly, these two features can be assigned to the symmetric and antisymmetric vibrations of "monomeric" water, respectively. Let us remind that the Raman scattering activity of totally symmetric vibrations is greater than that associated with antisymmetric vibrations, whereas the converse is true in infrared spectroscopy. This explains why the relative intensity of the two bands of water is reversed in the two spectroscopies (compare Figures 1 and 3). Therefore, the intense mode observed in Raman has to be assigned to the symmetric stretch of the molecule. The Raman profiles have been found to be nicely fitted by two Lorentzian profiles, and the band-shape parameters obtained are reported in Table 1. We notice that there is no spectral feature at low wavenumbers of ca. 3400 cm^{-1}. This finding supports the idea that the concentration of oligomers is certainly too weak to contribute significantly in the Raman profiles observed in the ν_{OH} spectral region. This is a consequence of the spectral contrast existing between the two techniques concerning the activities of spectral transitions belonging to small aggregates. We have shown on supercritical water and alcohols that infrared spectroscopy is particularly adapted to the study of oligomer formation in these fluids, whereas Raman scattering is more able to detect the so-called "free" species (monomeric and nonbonded OH vibrations in oligomers).[50,52−59]

II.3. Preliminary Discussion. First, we emphasize the good consistency existing between infrared and Raman scattering measurements. It is readily apparent from Table 1 that the two spectroscopic techniques lead, within experimental uncertainties, to the same values of the band centers positions for all of the systems investigated. This result supports the assignment proposed in terms of the ν_1 and ν_3 bands of "monomeric" water.

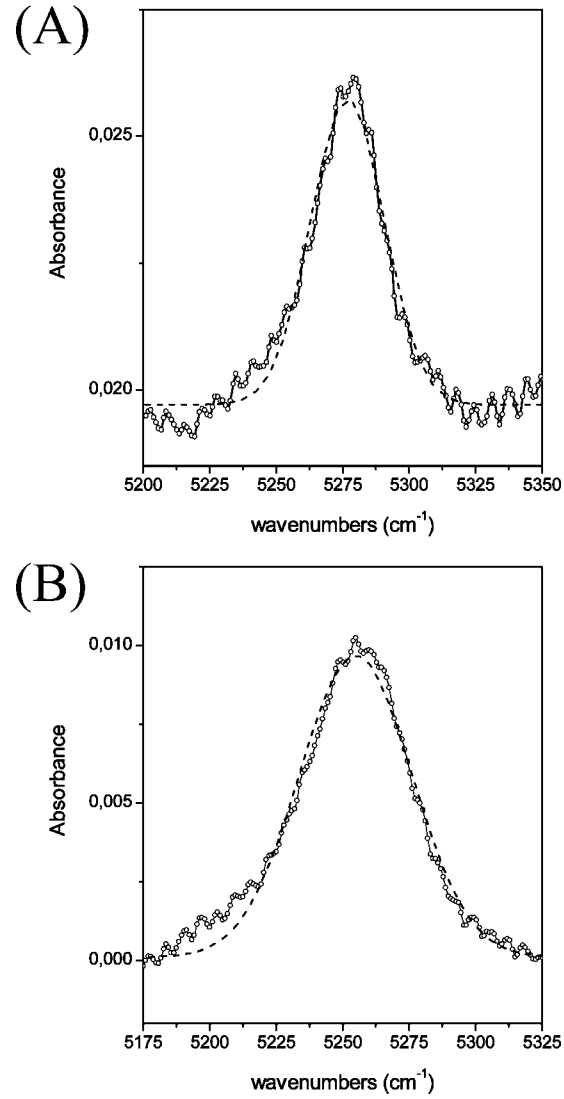

Figure 2. Measured (○) IR profile associated with the $\nu_2+\nu_3$ combination band (5200−5300 cm^{-1}) in the PF_6/B_{Mim} (A) and BF_4/B_{Mim} (B) mixtures (water content about 1% in volume) and corresponding fitted Gaussian profile (- - -).

Thus, within experimental uncertainties, the ν_1 symmetric stretch vibration is about 3563 cm^{-1} in B_{Mim}^+/BF_4^- and 3597 cm^{-1} in B_{Mim}^+/PF_6^-. For this latter system, the ν_3 antisymmetric stretch being also found at wavenumbers about 30 cm^{-1} (of 3640 cm^{-1}) higher than those in B_{Mim}^+/BF_4^- solution, the wavenumbers difference $\Delta\nu_{13} = \nu_3 - \nu_1$ is almost anion independent and lower than in gaseous water (about 99 cm^{-1}).[48,49] The red shifts of the two stretching modes and the decrease of $\Delta\nu_{13}$ as compared to those of gaseous water reveal that "monomeric" water undoubtedly interacts with its surrounding.

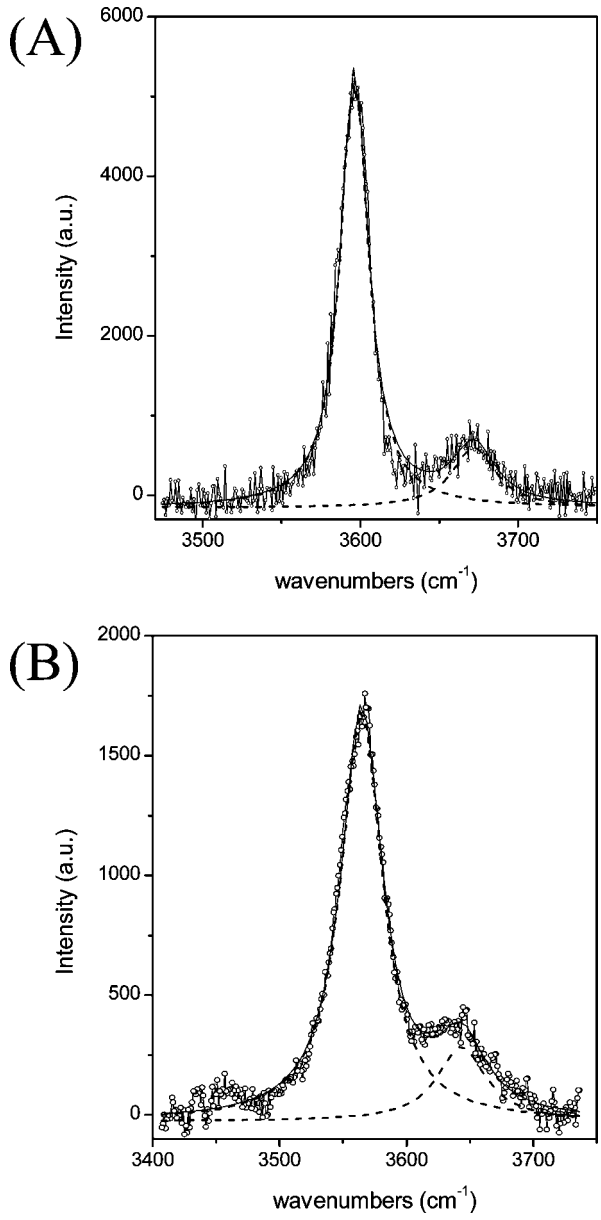

Figure 3. Measured (○) Raman spectra of water in the OH stretching modes region (3500−3800 cm^{-1}) in the PF_6/B_{Mim} (A) and BF_4/B_{Mim} (B) mixtures (water content about 1% in volume). (- - -) Fitted Lorentzian profiles.

Additional support about the existence of the interaction between water and ILs is provided upon examination of the full width at half-height (fwhh) of the observed profiles. Again, it is found (see Table 1) that the values of the widths measured in both techniques, if not identical, are nevertheless in fair agreement. Because polarized Raman profiles are mostly dependent upon vibrational relaxation whereas infrared band shapes depend upon both rotational and vibrational relaxation, we may also infer that water band shapes are mostly governed by the latter relaxation mechanism. This conclusion is consistent with the results obtained in our previous studies.[48,49] Indeed, it was found that when water interacts with a solvent, the rotational motion becomes more strongly and anisotropically hindered as the strength of the interaction increases, leading to IR profiles mostly governed by vibrational relaxation. This can be checked from a comparison of the fwhh of system (I), which displays almost the same spectral features as those found for water in benzene (which are of 20 and 32 cm^{-1} for the ν_1 and ν_3 modes, respectively[48]). However, a closer examination of width values (Table 1) shows that whereas widths are almost the same for system (I) they appear slightly greater than those measured for system (II). The differences, although small, are beyond our estimation of experimental uncertainties. We therefore suspect that these differences might be due to a contribution of rotational motions, which are not fully hindered and might contribute to the greater broadening observed in the IR profiles.

Comparing the broadening of the IR and Raman profiles between the two systems, we found that the widths are greater by a factor of 2 in B_{Mim}^{+}/BF_4^{-} solution. The band centers being also more red-shifted, we may correlate these findings with those reported in the literature for water dissolved in solvents of increasing H-bond strength.[60−62] Indeed, it has been experimentally found that as the strength of the interaction increases, profiles are more red-shifted and experience concomitantly a greater broadening. Although there are no definitive explanations of the origin of the observed broadening, it has been conjectured that this might be connected with the disorder of the hydrogen-bond environment of water. Moreover, the existence in imidazolium-based ILs of nanoscaled structural heterogeneities due to microphase segregation in polar/nonpolar domains might be a first step toward an interpretation about the widths of the vibrational bands associated with the OH stretches. In this context, an alternative explanation has been also proposed on the basis of consideration of the dynamics of hydrogen-bond formation−breakage.[63] Clearly, we are far from proposing here an explanation of this broadening. However, the relevant point for our purpose is that this correlation indicates that the strength of interaction of water with the surroundings is certainly greater in system (II) than in system (I).

One last intriguing question remains open and concerns the band shapes that are found different in infrared (Gaussian profiles) and in Raman (Lorentzian). This difference cannot be explained by arguing that the slow modulation condition of vibrational states applies in IR spectroscopy leading to Gaussian inhomogeneously broadened profiles, whereas in Raman spectroscopy a different regime has to be considered a fast modulation condition of the vibrational states leading to Lorentzian homogeneously broadened band shapes. We believe that the difference between the mathematical descriptions of band shape in the two spectroscopic techniques is pertinent. We surmise that this is certainly related to the fact that dipole transition derivative and transition polarizability derivative at the basis of the genesis of the IR and Raman spectra of water are differently affected by the environmental distribution. Such a viewpoint, which has been pointed out before, should deserve more theoretical understanding.[63]

The last spectroscopic observable to be discussed concerns the ratio of the intensities of the profiles $R = I\nu_3/I\nu_1$ (Table 1). In infrared spectroscopy, the R value varyies between 1.9 and 3.4 and strongly departs from that of water in the gaseous phase (for which $R = 14$). This ratio has been proven to be a strong indicator of the nature and strength of the interaction of water with its surroundings. As a matter of fact, we found in our previous IR studies of solitary water interacting through hydrogen bonding with a solvent as in liquid benzene that R strongly decreases ($R = 3.0$). In contrast, as water interacts with an electron donor−electron acceptor solvent, for example, water highly diluted in liquid hexafluorobenzene, the value $R = 11$ was found close to the gas-phase value.[48] Considering now Raman spectroscopy, we find that the values of R are about 0.16. This new finding has to be contrasted with the results reported on previous systems like water−benzene for which only

the ν_1 mode could be detected. Thus, we can come to the conclusion that in the systems investigated here, water interacts with ILs, and that on the basis of the shifts, the strength of interaction between water and ILs should be comparable to that observed for a weak hydrogen-bonded system such as water in benzene.[64−70] So, the scaling of the hydrogen-bond interaction strength of water in solvents based upon empirical spectroscopic criteria should be revised for ionic liquids.

It is important to compare our results with those reported by Kazarian et al. from their ATR infrared investigation of water diluted in ILs.[47] We do agree with the conclusions that water exists in IL under monomeric form (at low water contents) coexisting with small water aggregates (at higher water concentration). The band center positions and $\Delta\nu_{13} = \nu_3 - \nu_1$ are consistent in both studies and indeed reveal that monomeric water interacts with its surroundings. We were able to confirm also this viewpoint from a band-shape analysis comparing Raman and infrared profiles and also using information reported in our previous work as well. Because band centers are red-shifted with values greater than or equal to those reported in the water−benzene system (∼89 cm^{-1}), we may infer that the strength of the interaction in the IL investigated is greater than or comparable to that existing in water−benzene. We note that on the basis of all of the observables reported here and not only by considering the band center positions (as in reference), we could classify the systems according to the strength of interaction in the order system (I) < system (II). This classification agrees with that proposed by Kazarian et al.[47]

The nature of the interaction is more difficult to assess only on the experimental ground. Indeed, the band center positions and shifts are consistent with the signature of a hydrogen-bond interaction. However, in Raman spectroscopy, the activity of the ν_3 mode, which is not observed even for hydrogen-bonded water in molecular solvents, deserves to be further investigated. We may expect that the water molecule experiences the electric field of the anion and the cation while retaining its C_{2v} symmetry. As a consequence, the transition dipole moment and transition polarizability derivatives should be enhanced, giving rise in turn to enhanced intensity of the stretching modes in both spectroscopies. Such an explanation has been raised for an ionic aqueous solution of Na BF_4 for which the ν_3 mode of water has been observed in Raman spectroscopy.[71−73] However, this point of view has been further revisited by Scherer who provided an alternative explanation in which the activity of the mode is due to the formation of two H-bonds of water with two anions of the salt.[63] We believe that these physical insights need to be further theoretically investigated. The following part of this article will be devoted to studying the spectral signatures of water from DFT calculations in both systems in view to shed light on the nature of the interaction existing between water and the ions forming the ILs.

III. Modeling the Vibrational Spectra of Water in 1-Alkyl-3-methyl Imidazolium-Based ILs

We have carried out DFT calculations of water interacting with a series of cation−anion couples. Because calculations involving a realistic number of IL ions and water molecules would require intensive computer resources, we have idealized the system by supposing that the observed spectral signatures mainly result from interactions of water with a minimum of ions pairs. For that purpose, we have carried out the calculation by considering first a single water molecule interacting with one cation−anion pair and then with two cation−anion pairs. In addition, we have also assessed the influence of the alkyl chain length on the local structural organization and vibrational spectra of water interacting with the ion pairs by varying in the 1-alkyl, 3-methyl imidazolium cation the alkyl chemical group from methyl to octyl. In this context, it has been shown that the alkyl chain length has a big impact on the nanosegregated structure of the ILs.[37,74] Recently, CARS spectroscopic measurements have put in evidence mesoscopic local structures in imidazolium/hexafluorophosphate ILs and for which the spatial distribution varies with the alkyl chain length.[75]

For cations having short alkyl groups, the nanostructural organization is characterized by nonpolar domains dispersed in a polar network continuum. This situation corresponds to the so-called regime controlled by electrostatic interaction between the ions.[74] As the alkyl chain lengthens (C_7 or higher), the nanostructural organization progressively evolves toward a regime in which van der Waals interactions between the alkyl groups become predominant. In this situation, the charged groups form a polar network permeated by the nonpolar domains. As for the cohesive energy, it has been shown that it increases with the alkyl chain length.[76,77] In the present study, we consider a single water molecule, and we are mainly interested by the local organization of water and its consequences on the vibrational spectra. It can be easily anticipated that the solitary water molecule should be attached to the polar network and therefore should not be affected by the "swelling" of the nonpolar parts of the ILs as the alkyl chain length increases.

We have arbitrarily considered as a reference the local energy minimum structure of water interacting with the ion pair(s) involving the 1,3-dimethyl imidazolium cation (labeled as D_{Mim^+}). Indeed, this cation keeps the main chemical properties of the core with a minimum number of atoms. We considered water interactions with ion pairs involving the two distinct anions, the hexafluorophosphate anion $\{PF_6^-\}$ and the tetrafluoroborate anion $\{BF_4^-\}$. In this section, we focus on the calculated spectral features of water in the region of the symmetric ν_1(OH) and antisymmetric ν_3(OH) stretching modes (3300−3800 cm^{-1}). More precisely, we will consider the shifts and IR and Raman intensity variations of the peaks associated with the ν_1 and ν_3 stretches as well as the ν_2 bending mode of water as compared to those of isolated water. Other modes associated with either the anion or the cation of the ion pairs will be briefly discussed as being relevant to provide additional information about the nature of the water interactions in ILs.

III.1. Details of the Calculations. The quantum chemistry calculations have been carried out using the Gaussian 03 suite.[78] The optimized structures of water interacting with the (cation−anion) ion pairs have been achieved from the DFT procedure through the B3LYP functional using the 6-31+G(d,p) basis. It is now well-established that the B3-based DFT procedures provide a very cost-effective means of determining satisfactory harmonic vibrational transitions on a series of molecules in comparison with other procedures (B-based DFT or MP2 theory of perturbation).[79] The optimized geometries have been obtained using a very tight criterion of convergence. The detailed structures can be obtained from the authors upon request.

For water interaction with ion pairs or ion pair dimers, the calculated interaction energy (ΔE_{int}) was corrected from the basis set superposition error (BSSE) using the full counterpoise (CP) technique.[80] For water interacting with a cation−anion pair, the BSSE corrected binding energy has been obtained according to the site−site function counterpoise method (SSFC).[80−84] The vibrational analysis has been carried using the standard Wilson FG matrix formalism based on the harmonic force field

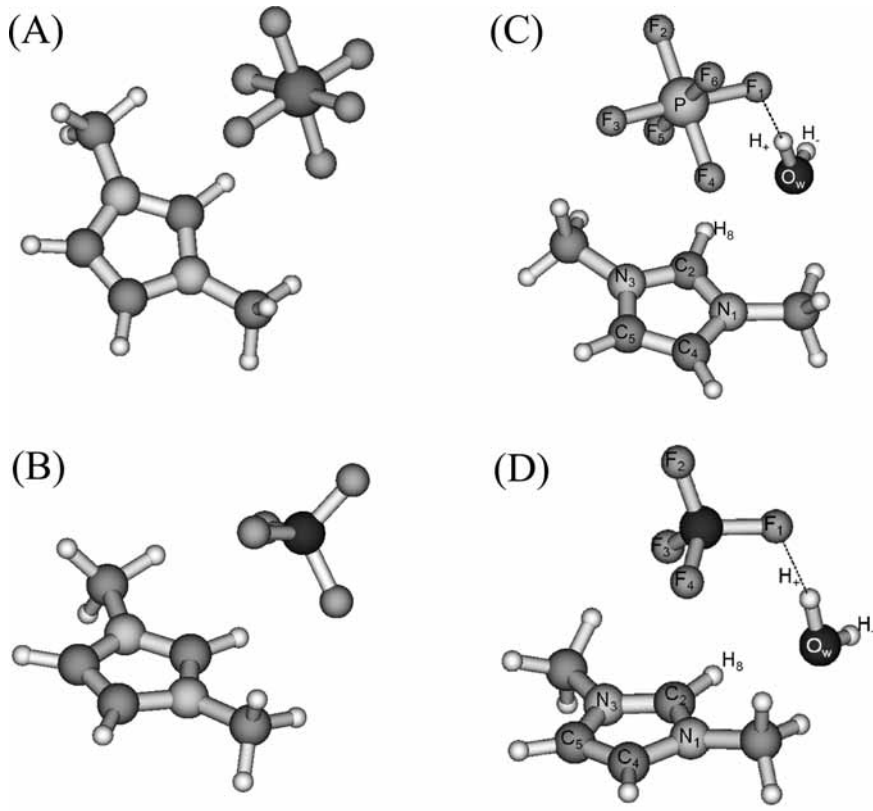

Figure 4. Calculated energy minimum structures of the "dry" ion pairs (A) $\{PF_6^- \cdot D_{Mim}^+\}$ and (B) $\{BF_4^- \cdot D_{Mim}^+\}$ and for water interacting with these single ion pairs (C) $\{PF_6^- \cdot D_{Mim}^+\}$ and (D) $\{BF_4^- \cdot D_{Mim}^+\}$.

approximation.[85] In this framework, the predicted vibrational transitions are usually overestimated as compared to the experimental band center positions due to the neglect of the anharmonicity effects. Scaling factors have been reported to take into account such effects and to facilitate comparison with experimental observed vibrational transitions. Suitable scaling factors for fundamental vibrations have been reported for different B3-DFT procedures using the 6-31G(d) basis set.[79,86,87] The scaling factor requested from the DFT-B3LYP procedure with the 6-31+G(d,p) basis set is of 0.964.[88]

III.2. Water Interacting with a Single Ion Pair. Considering water interacting with a single ion pair as representative of the local arrangement existing in ILs is undoubtedly an oversimplified picture of the real system. Such a treatment justified by the gain in computational resources will allow us to assess the drawback of the approach, which does not take into account the collective interaction mechanisms taking place in the first solvation shell of water in ILs and their consequences on the IR and Raman spectral features of water.

The ion pair formation is preliminary governed by the electrostatic forces for which the strength can be easily expected to be of 1 order of magnitude greater than that involved in the water−ion (cation or anion) interactions. In addition, other nonbonded interactions have been also invoked such as weak hydrogen-bond interactions between the F atoms of the $\{PF_6^-\}$ and $\{BF_4^-\}$ anions and the acidic $C_{(2)}H$ proton of the cation rings, especially in 1-alkyl-3-methyl imidazolium-based ionic liquids.[89−95] Water interactions with the anion−imidazolium cation couple involve a complex potential energy surface having numerous local energy minima. As a consequence, there are several possible structures for water interacting with one ion pair. However, a preliminarily survey of the calculated energy potential surfaces for water interacting with both $D_{Mim}^+ \cdots PF_6^-$ and $D_{Mim}^+ \cdots BF_4^-$ ion pairs (taken here as a reference system) allows us to privilege among them only the most energetically favorable structures. Therefore, we have selected among the calculated structures of water with the ion pair, the structure having the minimum value of energy.

III.2.1. Structure and Interaction Energy. First, we consider possible energy minimum structures of the isolated $\{D_{Mim}^+ \cdots PF_6^-\}$ and $\{D_{Mim}^+ \cdots BF_4^-\}$ ion pairs as displayed in Figure 4A and B. Globally, these calculated structures are found in good agreement with those reported in previous works (among the numerous other local energy minimum structures reached).[89−95] In our work, the values of the interaction energy of the $\{D_{Mim}^+ \cdots PF_6^-\}$ and $\{D_{Mim}^+ \cdots BF_4^-\}$ ion pairs are estimated at −79.0 and −84.9 kcal/mol, respectively. For the $\{B_{Mim}^+ \cdots PF_6^-\}$ and $\{B_{Mim}^+ \cdots BF_4^-\}$ ion pairs, the predicted structures are globally similar. Their calculated interaction energies (−77.7 and −83.3 kcal/mol, respectively) are found slightly increased (by less than 2%) due to the charge redistribution on the imidazolium ring (comparatively to the charge distribution on the D_{Mim}^+ cation). The increase of the cation alkyl chain upon the pair interaction energy is slightly destabilizing. Notice that our values are found in good agreement with those reported in literature.[90,96] We will consider now the influence of water interactions on the structure and the interaction energy of these ion pairs.

Possible structures of water interacting with the $\{D_{Mim}^+ \cdots PF_6^-\}$ and $\{D_{Mim}^+ \cdots BF_4^-\}$ ion pairs are also displayed in Figure 4C and D. In these structures, both protons of water are pointing away from the imidazolium ring, but only one of them forms a hydrogen bond with the nearest $F_{(1)}$ atom of the anions PF_6^- ($R_{H\cdots F}$ is 1.84 Å with PF_6^- and 1.72 Å with BF_4^-). In both structures, the $R_{O\cdots H}$ separation between the O atom of water and the most acidic proton $H_{(8)}$ of the imidazolium cation is about 2.1−2.2 Å. This suggests that in these structures water interacts with both partners of the anion−cation couple even if

TABLE 2: Calculated Fundamental Transitions ν_{cal} and IR and Raman Intensities of the Internal Modes of Water Interacting with a Single Ion Pair Involving Either PF_6^- or BF_4^- and Imidazolium Cations Having Different Alkyl Chain Lengths (D_{Mim}^+ and $C_{n}Mim^+$ (n = 2, 4))[a]

ν_{calc} (cm^{-1})	I_{IR} (km/mol)	I_{IR}/I°_{IR}	I_{Ram} (Å^4/amu)	I_{Ram}/I°_{Ram}	ν_{calc} (cm^{-1})	I_{IR} (km/mol)	I_{IR}/I°_{IR}	I_{Ram} (Å^4/amu)	I_{Ram}/I°_{Ram}	assignment
$\{PF_6^-\cdot D_{Mim}^+\}\cdot H_2O$					$\{BF_4^-\cdot D_{Mim}^+\}\cdot H_2O$					water modes
3891.9 (−38.5)	97.2	0.6	88.4	2.3	3893.8 (−36.6)	78.0	0.5	102.7	2.7	ν_3 (OH) str.
3637.5 (−170.6)	393.1	61.4	101.3	1.3	3512.9 (−295.2)	573.3	89.6	87.3	1.1	ν_1 (OH) str.
1662.0 (+59.0)	74.0	0.8	0.8	0.3	1663.5 (+60.5)	74.7	0.8	1.2	0.4	ν_2 (HOH) bend.
$\{PF_6^-\cdot C_{2Mim}^+\}\cdot H_2O$					$\{BF_4^-\cdot C_{2Mim}^+\}\cdot H_2O$					water modes
3891.4 (−39.0)	95.8	1.7	87.3	2.3	3893.5 (−36.9)	80.4	1.4	95.8	2.5	ν_3 (OH) str.
3644.2 (−163.9)	365.9	57.2	96.3	1.2	3558.7 (−249.4)	452.2	70.6	80.2	1.0	ν_1 (OH) str.
1660.4 (+57.3)	77.6	0.85	0.9	0.3	1654.1 (+51.0)	75.8	0.8	1.2	0.3	ν_2 (HOH) bend.
$\{PF_6^-\cdot C_{4Mim}^+\}\cdot H_2O$					$\{BF_4^-\cdot C_{4Mim}^+\}\cdot H_2O$					water modes
3901.6 (−28.8)	109.3	1.9	99.3	2.6	3892.3 (−38.1)	79.5	1.4	96.6	2.6	ν_3 (OH) str.
3668.6 (−139.5)	237.4	37.1	93.1	1.15	3572.9 (−235.2)	414.9	64.8	77.1	0.95	ν_1 (OH) str.
1640.1 (+37.1)	93.3	1.0	1.8	0.55	1655.8 (+52.8)	81.8	0.9	1.1	0.3	ν_2 (HOH) bend.

[a] The vibrational analysis is carried out from energy minimum structures predicted at the B3LYP/6-31+G** level. Also reported in this table are the predicted shifts (values in parentheses) and IR and Raman intensity variations comparatively with the calculated spectra for isolated water. Note that $B_{Mim}^+ = C_{4Mim}^+$ and $E_{Mim}^+ = C_{2Mim}^+$. I_{IR}/I°_{IR} and I_{Ram}/I°_{Ram} are, respectively, the IR and Raman intensity ratio estimates for a given vibrational transition of water interacting with an ion pair dimer over isolated water.

the interaction of water with the imidazolium ring does not have a specific H-bond nature.

For water interacting with $\{D_{Mim}^+\cdots PF_6^-\}$ and $\{D_{Mim}^+\cdots BF_4^-\}$, the total interaction energy $\Delta E_{int}(tot)^{(COR)}$ is −88.7 and −95.5 kcal/mol, respectively (BSSE-corrected values according to the SSFC scheme[81]). The predominant contribution to $\Delta E_{int}(tot)^{(COR)}$ mainly results from the pair cation−anion interaction energy (calculated values of −75.2 and −80.3 kcal/mol, respectively). As compared to the isolated ion pairs (or "dry" ion pairs), the presence of water has a destabilizing effect on the cation−anion interaction energy, which is slightly increased by about 5%.

The pair water−cation interaction energies have similar values in both $\{D_{Mim}^+\cdots PF_6^-\}$ and $\{D_{Mim}^+\cdots BF_4^-\}$ water structures (of −8.2 and −7.8 kcal/mol, respectively). In contrast, the pair water−anion interaction energy is found to be less stabilizing with PF_6^- (−5.2 kcal/mol) than with BF_4^- (−7.3 kcal/mol) even if globally the structures are similar.

The increase of the alkyl chain length has for main effect to modify by a few percents the anion−cation and water−cation interaction energies. Indeed, for water interacting with $\{B_{Mim}^+\cdots PF_6^-\}$ and $\{B_{Mim}^+\cdots BF_4^-\}$, the water−cation and water−anion interaction energies are now, respectively, −5.7 and −6.4 kcal/mol (with PF_6^-) and −6.0 and −7.9 kcal/mol (with BF_4^-). However, the calculated cation−anion interaction energy is nearly unchanged (−74.2 and −80.3 kcal/mol, respectively). For all of these structures, the 3-bodies interaction energy weakly contributes to the total interaction energy (by less than 1%).

III.2.2. Vibrational Analysis of Water. The calculated harmonic vibrational transitions and IR and Raman intensities associated with the three internal modes of water are given in Table 2 and compared to the calculated spectra for isolated water. In both structures, the ν_1 and ν_3 modes are found significantly shifted toward lower wavenumbers (red-shifted) as compared to the vibrational transitions of isolated water. In particular, the ν_1 mode is significantly red-shifted (171 cm^{-1} with PF_6^- and 295 cm^{-1} with BF_4^-), whereas the ν_3 mode is found slightly red-shifted (38 cm^{-1}). As a consequence, the separation $\Delta\nu_{13} = \nu_3 - \nu_1$ of water interacting with the $D_{Mim}^+\cdots BF_4^-$ is significantly greater (∼381 cm^{-1}) than that for water with $D_{Mim}^+\cdots PF_6^-$ (∼255 cm^{-1}). The IR intensity of the ν_1 mode of water interacting with the ion pair is enhanced by more than an order of magnitude for both anions but with intensity greater with the BF_4^- anion than with the PF_6^- one. In contrast, the IR intensity of the ν_3 mode is weakly affected by the interactions with the ion pair. The IR intensity of the ν_1 mode is greater than that of the ν_3 mode by factors of 4 (PF_6^-) and 7 (BF_4^-), respectively. In Raman spectroscopy, the intensity of the ν_3 mode is significantly enhanced by a factor varying from 2.3 $\{D_{Mim}^+\cdots PF_6^-\}$ to 2.7 $\{D_{Mim}^+\cdots BF_4^-\}$, whereas the intensity of the ν_1 mode is increased by at most 30%.

Water interactions with ion pair involving an imidazolium cation having a longer alkyl chain (3-ethyl and 3-butyl) provide spectral features similar to those found with the reference ion pairs $\{D_{Mim}^+\cdots PF_6^-\}$ and $\{D_{Mim}^+\cdots BF_4^-\}$ (cf., Table 2). The red-shift and the IR intensity enhancement of the stretching modes of water, which are well-established as semiphenomenological spectroscopic criteria of H-bonding systems,[61,97] reveal the H-bond nature of the interaction of water with a single ion pair in which water plays the role of a single proton donor (SD) (with an F-atom of the anion). Nevertheless, the predicted spectral features radically diverge with experimental findings (cf., Table 1). More precisely, the observed IR absorption profiles clearly show that the intensity of the ν_1 mode is always found less intense than the ν_3 one. In other terms, the predicted spectral features from a local organization of water involving asymmetrical water−anion H-bonded structure (through a quasi linear O−H···F interaction) are not representative of the solvation of water highly diluted in ILs.

This leads us to consider differently the local organization of water. In this context, water interactions involving anion−water−anion symmetrical structures keeping locally the C_{2v} symmetry of water have been already evoked in previous theoretical study regions[37−40] as well as from experiments.[39,41,42,46,47] Although these so-called H-bonded structures are not always found stable or with a stationary point, such water associations (involving the double proton donor character of water or DD water) lead also to $\Delta\nu_{13}$-values, which might be compatible and able to interpret the spectroscopic observables. Nevertheless, their vibrational analysis needs to be further reinvestigated by taking into account not only the difficulty related to the stability of these entities but also to the relative IR and Raman intensities of the stretching modes of water.

Incidentally, we have also investigated the spectral features from calculated structures of water interacting with a single

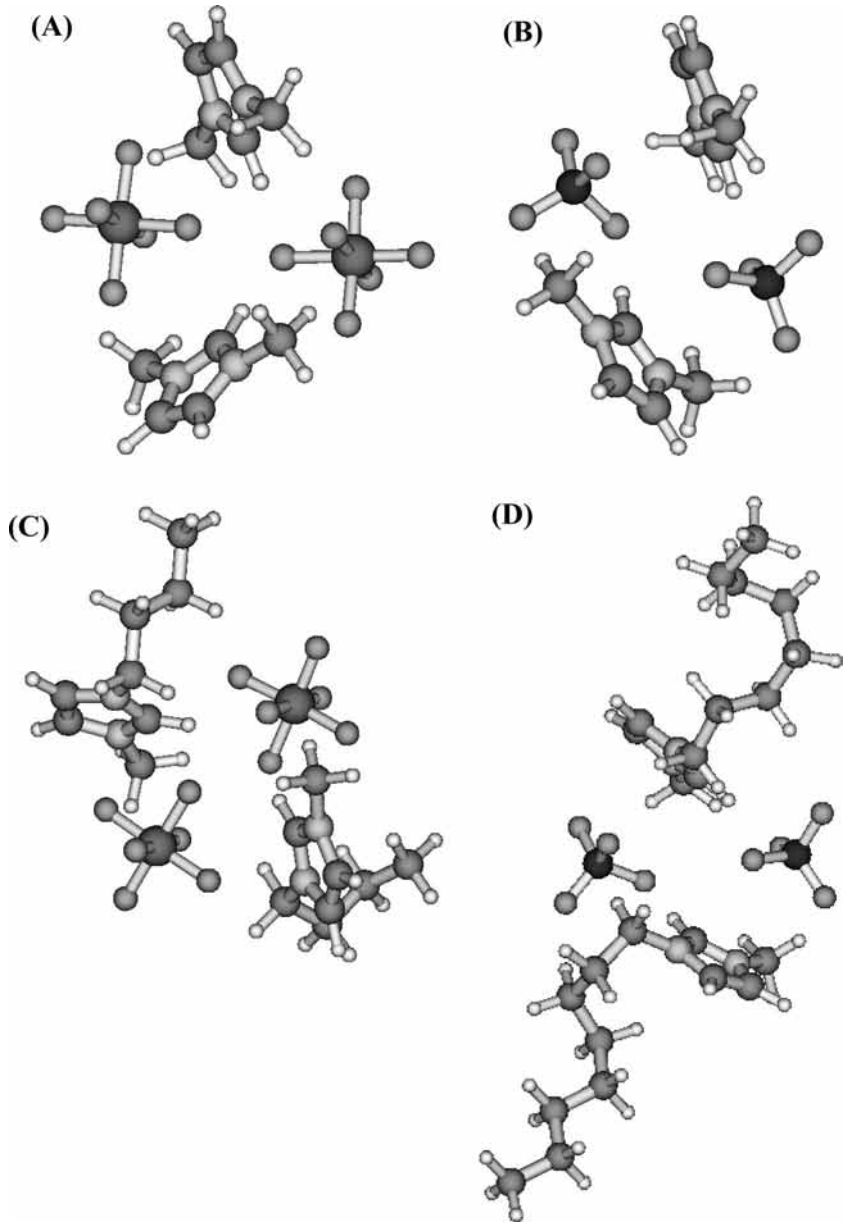

Figure 5. Local energy minimum structure of the ion pair dimers (A) $\{PF_6^- \cdot D_{Mim}^+\}_2$ and (B) $\{BF_4^- \cdot D_{Mim}^+\}_2$ calculated at the B3LYP/6-31+G** level. Idem scheme for ion pair dimers involving (C) 1-methy-3-butyl-imidazolium cations with PF_6^- and (D) 1-methy-3-octyl-imidazolium cations with BF_4^-.

anion (either BF_4 or PF_6, which are not discussed here). We found that these water complexes of 1:1 type are both stable and have a stationary point. More interesting, their separations $\Delta\nu_{13}$ are found to be ranging from 40 to 60 cm^{-1} and hence comparable to anion−water−anion symmetrical structures previously evoked to interpret the spectroscopic observables. Nevertheless, the calculated IR intensity ratio $R = I\nu_3/I\nu_1$ for a water molecule doubly hydrogen-bonded with a single anion leads to an intensity of the ν_1 stretch, which is greater than that of the ν_3 mode, that is, the reverse tendency of that observed in real water/ILs mixtures. In conclusion, we have to consider more sophisticated structures to reproduce qualitatively the main observed spectral signatures, keeping in mind that electrostatic (non additive) interactions possibly play a major role in the local organization taking place in water/ILs mixtures. This point will be further addressed in the following section.

III.3. Water Interacting with Ion Pair Dimer. ***III.3.1. Structure and Interaction Energy of the Ion Pair Dimer.*** First, we consider the structural organization of the "dry" ion pair dimers. As previously (section III.2), we survey possible structures of the ion pair dimers formed with two D_{Mim}^+−anion couples (either PF_6^- or BF_4^- anions). Again, the detailed potential energy surface due to the interactions within an isolated ion pair dimer is complex. As in the previous section (section III.2), we have searched ion pair dimer structures having the energy minimum.

Possible energy minimum structures of the ion pair dimers $\{D_{Mim}^+\cdots PF_6^-\}_2$ and $\{D_{Mim}^+\cdots BF_4^-\}_2$ are displayed in Figure 5. The ion pair dimer is organized to balance repulsive contributions (anion−anion and cation−cation interactions) and attractive cation−anion interactions. Within the ion pair, the minimum anion−anion distances are 6.0 Å ($D_{Mim}^+\cdots PF_6^-$) and 5.5 Å ($D_{Mim}^+\cdots BF_4^-$), whereas the distances between the

imidazolium rings are about 6.0−6.5 Å. The interatomic distances between the acidic H proton of the imidazolium rings and the nearest F atoms of the PF_6^- anions are typically ranging from 2.2 to 2.9 Å and about 2.0 Å with BF_4^- (distances greater than for single ion pairs, cf., section II.1).

Such a structural organization does not result from a simple superposition of the corresponding (isolated) ion pair structure. It necessarily involves non additive (many-bodies) interaction mechanisms leading to cooperative effects on both structural and energetic properties. From an energetic point of view, the non additive interactions signify that the total interaction (formation) energy between ions differs from the simple sum of the pair interaction energy contributions. It is possible to determine these different energy components (3- and 4-bodies interactions for an ion pair dimer) from our calculations by decomposing the total interaction energy according to the SSFC hierarchical scheme.[81,83]

The calculated 2-, 3-, and 4-bodies interaction energies ($\Delta E_{int}^{(n)}$, $n = 2$, 3, and 4) and total interaction energy $\Delta E(tot)_{int}^{(COR)}$ are reported in Table 3 (corrected from BSSE). The total interaction energy $\Delta E(tot)_{int}^{(COR)}$ is −192.9 and −205.5 kcal/mol for the $\{D_{Mim}^+\cdots PF_6^-\}_2$ and $\{D_{Mim}^+\cdots BF_4^-\}_2$ ion pair dimers, respectively. Although the two predicted structures are schematically comparable, the ion pair dimer involving BF_4^- anions is more stabilized than that with PF_6^-anions. The detailed decomposition of the total interaction energy shows that in both ion pair dimers, the pair interaction energy contributions predominate (90−95%), the pair anion−cation interaction energies $\Delta E_{int}^{(2)}$(An,Ca) being the main stabilizing factor. In contrast, the 3-bodies interaction energy contributions are rather destabilizing and originating mainly from the cation−anion−cation interaction process ($\Delta E_{int}^{(3)}$(Ca,An,Ca)). They represent less than 10% of the total interaction energy of the ion pair dimer. Finally, the 4-bodies interaction energy $\Delta E_{int}^{(4)}$ is a contribution weakly attractive (about −1.3 kcal/mol) and nearly independent of the nature of the anion.

The decomposition of the total interaction energy shows two significant entangled physical effects. The former concerns the cohesiveness of the ion pair dimer resulting from a balance between the attractive anion−cation interactions and the repulsive electrostatic forces between the ions having the same charge, which are "screened" by the presence of the counterions. The latter point concerns the destabilizing influence of the non additive interactions due to 3-bodies interactions in the ion pair dimers. These cooperative effects can be evaluated from the difference between the interaction energy a given oligomer (here a trimer) taken as an entity and the interaction energy of this oligomer involved in a higher size cluster. In our study, the cooperative effects have been estimated for the different cation−anion couples successively considered as an isolated entity and within the "dry" ion pair dimer. Thus, for instance, if we consider the ion pair dimers $\{D_{Mim}^+\cdots PF_6^-\}_2$ and $\{D_{Mim}^+\cdots BF_4^-\}_2$, the interaction energy of an anion−cation pair is −75.3 and −79.5 kcal/mol, respectively, instead of −79.0 and −84.9 kcal/mol for the corresponding isolated anion−cation pairs.

For ion pair dimers involving imidazolium cations having longer alkyl chain length, we notice qualitatively the same trends. As compared to the reference ion pair dimers, the structural organization is schematically found similar (cf., structures displayed in Figure 5C and D for $\{B_{Mim}^+\cdots PF_6^-\}_2$ and $\{O_{Mim}^+\cdots BF_4^-\}_2$). In particular, the anion−anion distance is nearly unchanged (6.0−6.1 Å with PF_6^- and 5.4−5.5 Å), whereas the relative distance between the two cations slightly increases as the alkyl chain lengthens. From the energetic point of view, the increase of the alkyl chain length has for main effect to weaken by a few percents the attractive anion−cation interaction energies due to the charge redistribution of the imidazolium rings (as compared to D_{Mim}^+). However, this cation−anion pair interaction component constitutes the predominant contribution to the stabilization of the different ion pair dimers as for the reference ion pair dimers. Moreover, a similar cooperative phenomenon on this interaction energy component can be quantified in the stabilizing mechanism of the ion pair dimer by comparison with the same component for the isolated anion−cation couple (with ion pairs involving B_{Mim}^+ for instance). As a consequence, the total interaction (formation) energy $\Delta E(tot)_{int}^{(COR)}$ of the ion pair dimers increases with the alkyl chain length of the imidazolium rings (and becomes less stable). The energy deviations from the reference ion pair dimers ions ($\{D_{Mim}^+\cdots PF_6^-\}_2$ and $\{D_{Mim}^+\cdots BF_4^-\}_2$) are found quite comparable for the PF_6^- and BF_4^- anions. Again, the 3-bodies interaction energy terms are repulsive (Table 3), whereas the 4-bodies interaction energy is found attractive and independent of the cation alkyl chain length.

III.3.2. Structure and Interaction Energy of Water Association with the Ion Pair Dimer. The local energy minimum structures of water interacting with the $\{D_{Mim}^+\cdots PF_6^-\}_2$ and $\{D_{Mim}^+\cdots BF_4^-\}_2$ ion pair dimers are displayed in Figure 6. In these structures, water preferentially interacts with the two anions (PF_6^- or BF_4^-) and forms nearly symmetric structures (A···H−O−H···A) in which each proton of water interacts with an F-atom. In this structural organization, the water plays the role of a proton double donor (DD water). The H···F interatomic distances $R_{H\cdots F}$ are about 1.98 Å (with PF_6^-) and 1.88 Å (with BF_4^-), that is, values slightly greater than those found for water interacting with the single ion pair. It is noteworthy that for water interacting with $\{D_{Mim}^+\cdots BF_4^-\}_2$, the calculated H···F interatomic distances are nevertheless significantly lower than those found in the unstable optimized structure for water interacting with only two anions.[98,99] Moreover, water does not exhibit any specific interaction with imidazolium rings.

As for the "dry" ion pair dimers, the total interaction energy $\Delta E(tot)_{int}^{(COR)}$ of water interacting with different ion pair dimers has been decomposed in terms of many-bodies interaction energy components ($\Delta E_{int}^{(n)}$, $n = 2$, 3, 4, and 5). As compared to the interaction energy analysis carried out for the "dry" ion pair dimers, the many-bodies interaction energy components are decomposed in interaction processes between ions (2-, 3-, and 4-bodies) and between water and the ionic species (2-, 3-, 4-, and 5-bodies). The calculated values of these different components have been reported in Table 3.

First, we consider the interaction energy decomposition for water associations with the ion pair dimers $\{D_{Mim}^+\cdots PF_6^-\}_2$ and $\{D_{Mim}^+\cdots BF_4^-\}_2$. The BSSE-corrected total interaction (formation) energy $\Delta E(tot)_{int}^{(COR)}$ is −182.4 and −200.4 kcal/mol, respectively. The examination of the different interaction energy components (Table 3) shows that the pair cation−anion interaction energy $\Delta E_{int}^{(2)}$(An,Ca) is the predominant attractive energy contribution to $\Delta E(tot)_{int}^{(COR)}$ (of −180.5 and −202.5 kcal/mol, respectively). As compared to the calculated values found for the "dry" ion pair dimers, the presence of water slightly weakens the interaction energy within the ion pair dimer. This perturbation is found greater for water interacting with PF_6^- than with BF_4^- (energy variations +8.4 and +1.9 kcal/mol, respectively).

TABLE 3: Calculated Total Interaction Energy and Pair and 3-, 4-, and 5-Bodies Interaction Energies for the Structures of Water Interacting with an Ion Pair Dimer Involving Imidazolium Cations Having Different Alkyl Chain Length with PF_6^- and BF_4^- Anions[a]

	$\{PF_6^-\cdot D_{Mim}^+\}_2$	$+H_2O$	$\{PF_6^-\cdot E_{Mim}^+\}_2$	$+H_2O$	$\{PF_6^-\cdot B_{Mim}^+\}_2$	$+H_2O$	$\{PF_6^-\cdot O_{Mim}^+\}_2$	$+H_2O$	$\{BF_4^-\cdot D_{Mim}^+\}_2$	$+H_2O$	$\{BF_4^-\cdot E_{Mim}^+\}_2$	$+H_2O$	$\{BF_4^-\cdot B_{Mim}^+\}_2$	$+H_2O$	$\{BF_4^-\cdot O_{Mim}^+\}_2$	$+H_2O$
Ionic Interactions																
ΔE_{int}(ions)	−177.7	−169.3	−175.6	−169.9	−173.1	−168.0	−171.8	−168.1	−189.6	−187.7	−186.6	−184.7	−185.6	−182.1	−184.1	−180.9
$\Delta E_{int}^{(2)}$	−192.9	−180.5	−191.2	−182.2	−188.6	−180.5	−187.6	−180.7	−205.5	−202.1	−203.5	−199.7	−202.5	−196.0	−201.3	−194.7
$\Delta E_{int}^{(2)}$(An,Ca)	−301.2	−277.0	−299.3	−284.0	−294.9	−281.3	−292.6	−281.4	−317.9	−310.6	−307.0	−304.8	−309.8	−303.9	−307.2	−301.2
$\Delta E_{int}^{(2)}$(An,An)	+57.0	+53.2	+57.8	+56.9	+57.4	+56.9	+57.4	+57.2	+61.2	+59.8	+54.3	+57.5	+57.6	+61.3	+57.3	+61.1
$\Delta E_{int}^{(3)}$	+16.5	+12.0	+16.9	+13.3	+16.8	+13.3	+17.0	+13.4	+17.2	+15.6	+18.3	+16.2	+18.3	+14.5	+18.2	+14.6
$\Delta E_{int}^{(3)}$(An,An,Ca)	+4.7	+2.5	+3.6	+2.6	+2.7	+1.7	+1.6	+1.0	+3.5	+3.9	+5.9	+4.2	+2.6	+1.1	+1.6	+0.4
$\Delta E_{int}^{(3)}$(Ca,An,Ca)	+11.8	+9.5	+13.3	+10.6	+14.1	+11.6	+15.4	+12.6	+13.6	+11.7	+12.4	+11.9	+15.6	+13.4	+16.7	+15.1
$\Delta E_{int}^{(4)}$	−1.3	−0.8	−1.3	−0.9	−1.3	−0.9	−1.2	−0.8	−1.3	−1.1	−1.4	−1.2	−1.2	−0.9	−1.1	−0.9
Water−Ions Interactions																
ΔE_{int}(H_2O-ions)		−13.1		−12.6		−12.6		−12.0		−12.8		−13.4		−12.2		−11.9
$\Delta E_{int}^{(2)}$		−14.8		−14.8		−14.8		−14.4		−18.2		−17.8		−17.8		−17.5
$\Delta E_{int}^{(2)}$ (H_2O−An)		−11.6		−14.4		−14.4		−14.5		−20.5		−20.4		−21.1		−21.1
$\Delta E_{int}^{(3)}$		+2.2		+2.8		+2.8		+3.0		+6.5		+6.5		+6.4		+6.4
$\Delta E_{int}^{(3)}$(An,H_2O,An)		+1.8		+1.9		+1.9		+1.9		+2.0		+2.1		+2.3		+2.3
$\Delta E_{int}^{(3)}$(An,H_2O,Ca)		∼0		+0.4		+0.4		+0.4		+4.1		+4.4		+3.6		+3.7
$\Delta E_{int}^{(4)}$		−0.6		−0.7		−0.7		−0.6		−1.2		−1.2		−0.9		−0.9
$\Delta E_{int}^{(5)}$		∼0		+0.1		+0.1		+0.1		+0.1				+0.1		+0.1
Total Interaction Energy																
ΔE_{int}(tot)		−182.4		−182.5		−180.6		−180.1		−200.5		−198.1		−194.3		−192.8
Association Energy ΔE_{as} and Enthalpy																
ΔE_{as}(H_2O)		−4.7		−6.9		−7.5		−8.3		−10.9		−11.5		−8.7		−8.7
$\Delta E_{as}(H_2O)^{(+ZPE)}$		−3.9		−6.3		−6.4		−6.7		−9.0		−10.0		−7.4		−6.0
$\Delta H_f(T_{298K})$		−4.5		−7.0		−7.1		−7.3		−10.8		−10.8		−8.0		−6.6

[a] Interaction energy components between ions are compared to those obtained for the "dry" ion pair dimer [B3LYP/6-31+G(p,d)]. The calculated energies (in kcal/mol unit) have been corrected from BSSE according to the SSFC scheme.[81,83] Notice that $E_{Mim}^+ = C_{2Mim}^+$, $B_{Mim}^+ = C_{4Mim}^+$, and $O_{Mim}^+ = C_{8Mim}^+$.

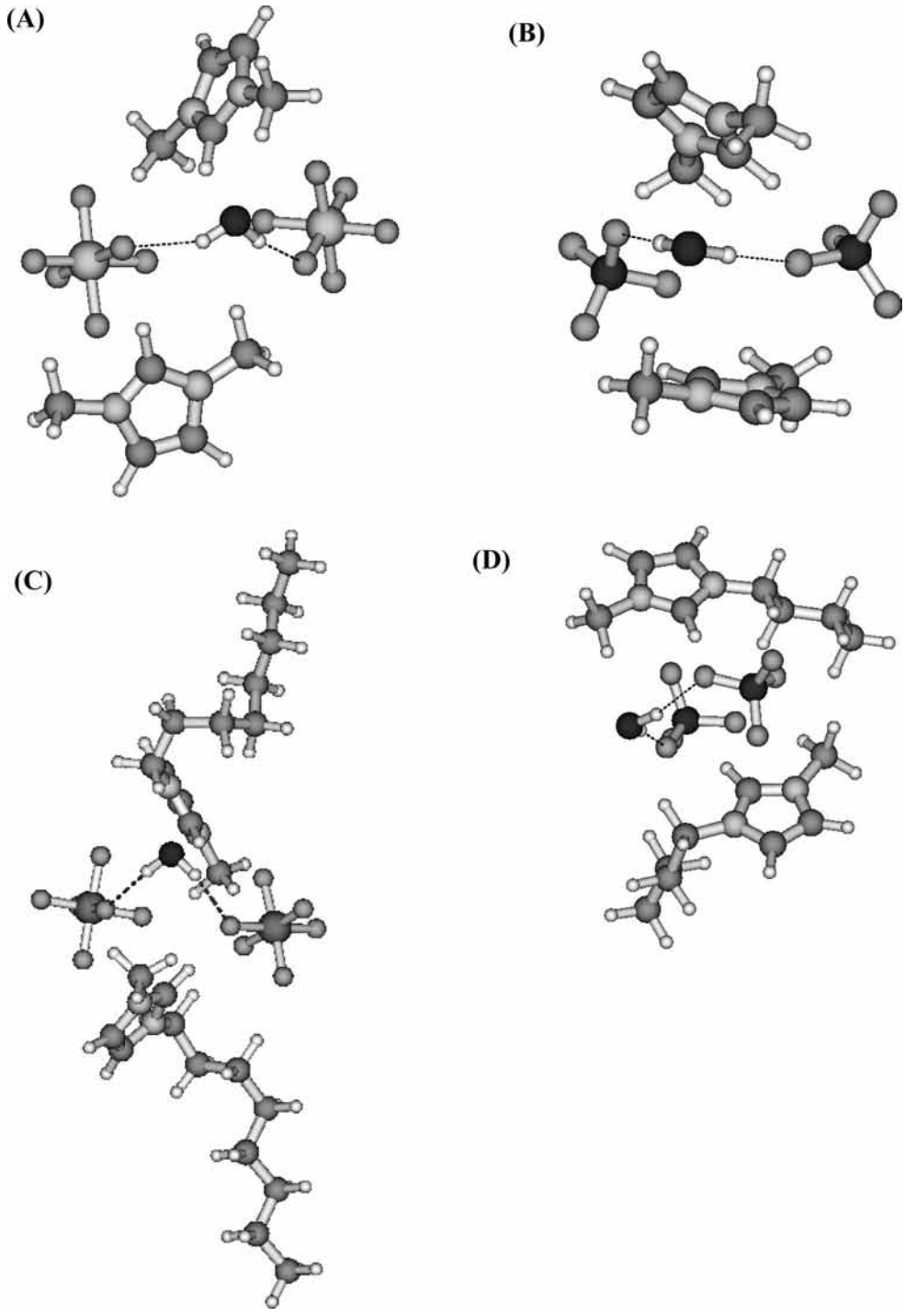

Figure 6. Local energy minimum structure of water interacting with the ion pair dimers (A) $\{PF_6^- \cdot D_{Mim}^+\}_2$ and (B) $\{BF_4^- \cdot D_{Mim}^+\}_2$ calculated at the B3LYP/6-31+G** level. Idem scheme for ion pair dimers involving (C) 1-methy-3-octyl-imidazolium cations with PF_6^- and (D) 1-methy-3-butyl-imidazolium cations with BF_4^-.

The 3-bodies interaction energy components between ions as well as between water and the ions are found again as destabilizing contributions (less than 10%) to the interaction energy, whereas the 4-bodies interaction energy components $\Delta E_{int}^{(4)}$ are attractive and weak (about −1.5 to −2.0 kcal/mol).

The examination of the different water−ions interaction energy components (Table 3) shows that the pair water−anion interaction energy $\Delta E(H_2O-An)_{int}^{(2,COR)}$, which constitutes the main attractive contribution, is greater for water interacting with BF_4^- than with PF_6^-, whereas the water−ion interaction energy components $\Delta E_{int}(H_2O\text{-ions})$ are estimated with quite comparable values (cf., Table 3). This results from a compensative effect originating from 3-bodies interactions between water and the ions. These non additive interactions represent a non negligible contribution (about 20−30%) to the interaction energy of water with the ion pair dimers $\{D_{Mim}^+ \cdots PF_6^-\}_2$ and $\{D_{Mim}^+ \cdots BF_4^-\}_2$.

For water interactions with ion pair dimers involving imidazolium cations having a longer alkyl chain, we obtain from the energetic point of view the same trends as those reported for water interacting with $\{D_{Mim}^+ \cdots PF_6^-\}_2$ and $\{D_{Mim}^+ \cdots BF_4^-\}_2$. Increasing the alkyl chain mainly weakens (by a few percents) the interaction energy between ions, modifying the charge distribution on the imidazolium rings.

To conclude, non additive (3-bodies) interactions play a determining role in the local organization of water with the ion pair dimers. They lead to a cooperative effect between ionic species, which does not favor and even screen the interactions of a water molecule with acidic proton of the imidazolium rings at low water concentration. Moreover, non additive interactions are also involved in the solvation mechanism of water in ILs. They mainly originate from the repulsive electrostatic forces between the O atom of water and the F atoms of the two anions (PF_6^- or BF_4^-). In that sense, the subtle balance between electrostatic interactions (both repulsive and attractive) due to the ionic species and the general trend of water protons to form F···H hydrogen-bond (attractive) interactions with PF_6^- or BF_4^- anions plays a determining role by favoring nearly "symmetric" A···H−O−H···A structures. In such structures, the F···H−O hydrogen-bond interactions formed are found nevertheless less directional than those usually formed in molecular solvents (angular deviations about 10−15° from a collinear arrangement), although the F···H distances are typically about 1.9−2.0 Å. Comparable angular deviations in the intermolecular hydrogen-bonding interactions of water with fluorinated anions have been recently reported in MD simulations of water diluted in ILs.[100−102]

The water−(anions and cations) interaction energy is obviously insufficient to break down the cohesion of the ion pair dimer. Indeed, the calculated energy interaction of water attached to the polar network (via two anions) is found ranging from −12 to −13 kcal/mol as compared to interaction energy estimates between the ions ranging from −187.0 to −193.0 kcal/mol and from −201.0 to −206.0 kcal/mol for "dry" ion pair dimers involving PF_6^- and BF_4^- anions, respectively (cf., Table 2). Nevertheless, in the presence of water, the interaction energy of the ion pair dimers ΔE_{int}(ions) becomes less stable even if it is only varied by a few percents (less than 5%) as compared to that of the "dry" ion pair dimer (cf., Table 3). More precisely, this interaction energy difference becomes a significant contribution as included in the variation of the total interaction energy $\Delta(\Delta E_{int}(tot))$ under the transformation "wet" ← "dry" ion pairs dimers (cf., Table 3). This quantity corresponds to a "gas-phase" association energy of water $\Delta E_{ass}(H_2O)$ of about −6.4 kcal/mol with PF_6^- anions and varying from −6.0 to −10.0 kcal/mol with BF_4^- anions. These calculated energy values allow us to establish a water−anion interaction strength scale, which approximately follows the hierarchy proposed by S. Kazarian from ATR-IR measurements, $[PF_6^-] < [BF_4^-]$.[47] It is noteworthy that the zero point energy (ZPE) correction is non negligible in the evaluation of $\Delta E_{ass}^{(+ZPE)}$ as well as in the corresponding (formation) enthalpy estimates ΔH_f at room temperature (cf., Table 3).

In the following section, we will investigate if such symmetric water associations (A···H−O−H···A) can rationalize the specific spectral features observed in real solutions of water diluted in ILs.

III.3.3. Predicted IR Absorption and Raman Spectra. Vibrational Modes of Water. The calculated vibrational transitions and IR and Raman intensities of the internal modes of water interacting with the different ion pair dimers are reported in Table 4. It is noteworthy that the anharmonicity effects on these modes are considered using the scaling factor of 0.964. The scaled positions are found in fairly good agreement with the experimental values (cf., Table 1). The predicted vibrational spectra exhibit features that qualitatively correspond with the observed profiles of water (PF_6^- or BF_4^-/B_{Mim} solutions).

The two stretching modes of water are found red-shifted for both anions (PF_6^- and BF_4^-) as compared to the corresponding vibrational transitions of isolated water. The ν_1 mode is red-shifted by about 80−88 cm^{-1} (with PF_6^-) and 110−130 cm^{-1} (with BF_4^-). This red-shift increases with the water−anion strength. The ν_3 mode of water is also red-shifted. However, the shift is found greater than that experienced by the ν_1 mode (90−120 cm^{-1} with PF_6^- and 140−160 cm^{-1} with BF_4^- anions, cf., Table 4). As a consequence, the calculated separation $\Delta\nu_{13}$ is now found in fair agreement with experimental values (about 80 cm^{-1} after scaling).

The IR intensities of the ν_1 and ν_3 stretches are significantly enhanced with a ratio R_{IR} ranging from 1.4 to 2.6 with PF_6^- and from 1.8 to 3.4 with BF_4^-, respectively. The Raman intensity of the ν_1 and ν_3 modes is enhanced by 30−40% for water interacting with ion pair dimer involving PF_6^- anions. In contrast, it varies by 10−20% as water interacts with BF_4^- anions (Table 4). Finally, the intensity ratio R estimates confirm the overall trend experimentally observed (cf., Tables 1 and 4). In IR spectroscopy, the intensity of the ν_3 mode is found greater than that of the ν_1 mode ($R > 1$). In Raman spectroscopy, the calculations support the fact that the ν_3 mode is found with a noticeable intensity even if the calculated intensity values (and R-estimates) appear slightly overestimated as compared to those evaluated from the measured profiles. Nevertheless, they are found quite comparable to those reported from measured profiles (Table 1) within the computational and experimental uncertainties. The small discrepancies obtained between the predicted and measured $\Delta\nu_{13}$ and R values can originate from the quality of the basis set used in our calculations, but are more likely due to methodological limitations related to the low number of degrees of freedom involved in the calculated structures of water interacting with an ion pair dimer.

Despite such restrictions (as well as those related to a non explicit treatment of the anharmonicity effects), the predicted spectral signatures of water (shifts, separation of the OH stretches, and IR and Raman intensity ratios) are qualitatively in good agreement with the measured IR and Raman profiles (cf., Figure 7, scaled vibrational transitions). This establishes a relationship between observed spectral features and the water associations at the molecular level. Clearly, the predicted nearly symmetrical (A···H−O−H···A) structure appears as being representative of situations encountered in real solutions ILs and allows us to understand the main observed spectral features of water highly diluted in 1-alkyl-3-methyl imidazolium involving PF_6^- or BF_4^- anions. In such structures, the water molecule keeps locally a C_{2v} symmetry. Therefore, the OH bonds of water are found to be equally and likely less perturbed by interactions with two anions than by perturbations that should result from H-bond interactions of water with a single anion in asymmetric associations.

Interactions of water forming a single H-bond with F-atoms of the anions as well as interactions of water doubly hydrogen-bonded with a single anion are certainly not favored for water diluted in ILs (at low water concentration). Such associations lead to predicted IR spectral signatures of water (shifts and IR intensities) radically different from those observed. In particular, the IR intensity of the ν_1 OH stretch of water is found greater than that of the ν_3 mode, and the calculated IR intensity ratio R estimates exhibit the reverse tendency from that observed in real water/ILs mixtures.

The appearance of a band associated with the ν_3 modes of water in Raman scattering is related to a significant intensity enhancement, which is even not observed in usual H-bond

TABLE 4: Calculated Fundamental Transitions ν_{cal} and IR and Raman Intensities of the Internal Modes of Water Interacting with Ion Pair Dimers Involving the PF_6^- and BF_4^- Anions and Imidazolium Cations Having Different Alkyl Chain Lengths (D_{Mim}^+ and C_nMim^+ (n = 2, 4, and 8)) [B3LYP/6-31+G]**

ν_{calc} (cm^{-1})	I_{IR} (km/mol)	I_{IR}/I°_{IR}	I_{Ram} (Å^4/amu)	I_{Ram}/I°_{Ram}	assignment water modes[a]
					$H_2O\cdot\{PF_6^-\cdot D_{Mim}^+\}_2$
3841.1 (−89.3)	307.1	5.3	48.9	1.3	ν_3 (OH) str.
3728.2 (−79.9)	116.7	18.2	109.5	1.4	ν_1 (OH) str.
1634.9 (+31.8)	63.1	0.7	1.0	0.3	ν_2 (HOH) bend.
					$H_2O\cdot\{PF_6^-\cdot C_{2Mim}^+\}_2$
3819.0 (−111.4)	324.1	5.7	53.0	1.4	ν_3 (OH) str.
3723.5 (−84.6)	153.6	24.0	110.5	1.4	ν_1 (OH) str.
1653.9 (+50.8)	76.5	0.85	1.1	0.35	ν_2 (HOH) bend
					$H_2O\cdot\{PF_6^-\cdot C_{4Mim}^+\}_2$
3816.4 (−114.0)	317.6	5.5	51.6	1.4	ν_3 (OH) str.
3721.6 (−86.5)	159.7	25.0	111.2	1.4	ν_1 (OH) str.
1653.8 (+50.7)	79.1	0.9	1.1	0.35	ν_2 (HOH) bend.
					$H_2O\cdot\{PF_6^-\cdot C_{8Mim}^+\}_2$
3814.0 (−116.4)	274.3	4.8	53.2	1.4	ν_3 (OH) str.
3723.3 (−84.8)	191.0	29.8	118.0	1.45	ν_1 (OH) str.
1662.2 (+59.1)	117.0	1.3	2.15	0.65	ν_2 (HOH) bend.
					$H_2O\cdot\{BF_4^-\cdot D_{Mim}^+\}_2$
3785.9 (−144.5)	267.1	4.7	30.9	0.8	ν_3 (OH) str.
3697.7 (−110.4)	147.4	23.0	72.3	0.9	ν_1 (OH) str.
1664.1 (+61.0)	60.4	0.7	0.3	0.1	ν_2 (HOH) bend.
					$H_2O\cdot\{BF_4^-\cdot C_{2Mim}^+\}_2$
3787.8 (−142.6)	278.3	4.9	23.1	0.6	ν_3 (OH) str.
3700.4 (−107.7)	82.8	12.9	71.1	0.9	ν_1 (OH) str.
1653.8 (+50.7)	41.1	0.45	0.24	0.07	ν_2 (HOH) bend.
					$H_2O\cdot\{BF_4^-\cdot C_{4Mim}^+\}_2$
3769.8 (−160.6)	337.5	5.9	33.1	0.9	ν_3 (OH) str.
3681.9 (−126.2)	136.2	20.1	89.4	1.2	ν_1 (OH) str.
1661.3 (+58.2)	84.4	0.9	0.2	0.07	ν_2 (HOH) bend.
					$H_2O\cdot\{BF_4^-\cdot C_{8Mim}^+\}_2$
3769.1 (−161.3)	339.7	5.9	29.5	0.8	ν_3 (OH) str.
3680.5 (−127.6)	116.2	18.2	92.6	1.15	ν_1 (OH) str.
1661.3 (+58.2)	74.4	0.82	0.13	0.04	ν_2 (HOH) bend.

[a] I_{IR}/I°_{IR} and I_{Ram}/I°_{Ram} are, respectively, the IR and Raman intensity ratio estimates for a given vibrational transition of water interacting with an ion pair dimer over isolated water. The predicted shifts are given in parentheses.

interactions of water diluted in molecular solvents. This activity is likely induced by the polarization of water under the influence of the local electric field due to surrounding ionic species. Thus, we emphasize that H-bond water−anion interactions in ILs involve undoubtedly a more significant electrostatic character than for H-bond interactions (known to be mostly of electrostatic origin) of water in molecular systems.

The main spectral signatures of water do not appear influenced by the alkyl chain length of the imidazolium cations involved in the ion pair dimer. This does not contradict the well-established fact that the alkyl chain length of imidazolium cation has a significant impact on the nanosegregated structure in ILs.[37,103] Nevertheless, it can be easily supposed that in the regime controlled by electrostatic interactions, the (short length) alkyl chain of the imidazolium cations has no real influence on the local organization of water. For diluted water/IL solutions, "monomeric" water remains attached to the polar network via hydrogen-bond formation with two anions. As the alkyl chain increases, the nanostructural organization evolves toward a regime controlled by van der Waals interactions between the alkyl groups, that is, a structural organization in ILs in which the polar network is permeated by the nonpolar domains. Thus, the closest environment of water (polar domains in the ILs) should not be affected by the "swelling" of the nonpolar domains of the ILs as attested by our spectroscopic observations. However, the interpenetration of the expanding nonpolar domains through the tridimensional polar network could explain the increasing hydrophobic behavior of the ILs with the alkyl chain length.[12]

We conclude from these findings that the spectral signatures associated with the OH stretches of water are closely related to the double proton donor (DD) character of water interacting with two anions. To achieve our vibrational analysis of the internal modes of water, we notice that the ν_2 bending mode of DD water is found blue-shifted upon the formation of the symmetric A···H−O−H···A structure with two anions (either PF_6^- or BF_4^-).

Symmetric Stretches of the Anions. Water associations involving preferentially symmetric A···H−O−H···A structures could suggest likely spectral features associated with the symmetric stretches of the anions. The calculated vibrational transitions associated with the symmetric PF and BF stretches of the PF_6^- or BF_4^- anions engaged with different ion pair dimers (involving B_{Mim}^+ and O_{Mim}^+) are reported in Table 5 and compared to those evaluated in the presence of water interactions. These stretching modes, which from symmetrical considerations should be only Raman active for the hypothetical isolated anions, also exhibit an induced IR absorption (forbidden transition) activity within the ion pair dimer. In the presence of water interactions, these modes are predicted weakly blue-shifted by a few wavenumbers (<5 cm^{-1}). Recent Raman measurements in B_{Mim}/BF_4 mixtures have provided evidence for such an evolution of the band center position of the band associated with the BF stretching mode with the concentration of water.[42]

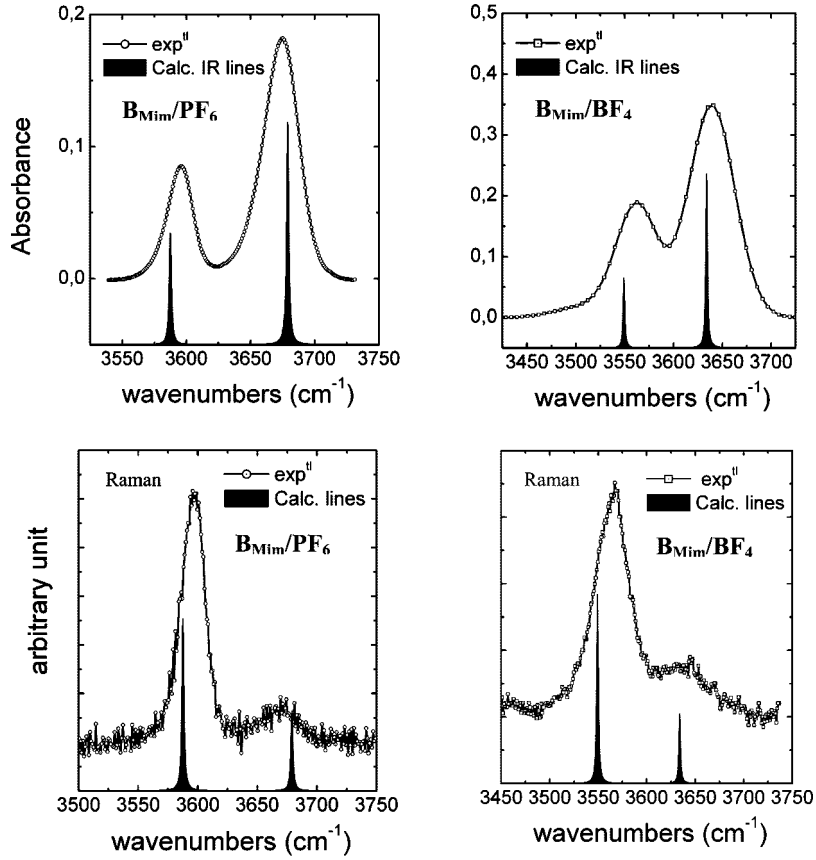

Figure 7. Comparison between measured IR and Raman spectra of water diluted in PF_6/B_{Mim} and BF_4/B_{Mim} mixtures and the corresponding lines calculated at the B3LYP/6-31+G** level (the scaling factor is 0.964[88]). For comparison, the IR intensity of the calculated lines is scaled by a factor 600 (PF_6) and 375 (BF_4), and the calculated Raman lines by a factor 100.

CH Stretches of the Imidazolium Rings. The CH stretching modes of the imidazolium rings have been considered as relevant vibrational probes of the interactions in ILs involving the most acidic proton of the imidazolium rings with F atoms of the PF_6^- or BF_4^- anions.[89,92−94,104] The presence of water in ionic liquids could lead to significant modifications in this spectral region (3000−3200 cm^{-1}).

The detailed assignment of the ring CH stretches is well-established in neat ("dry") PF_6^- and BF_4^- ILs. In particular, the CH stretches associated with the HCCH group of the imidazolium rings involved both higher wavenumbers symmetric and lower wavenumbers antisymmetric components (3100−3200 cm^{-1}). The CH stretching mode associated with the cation $NC_2(H)N$ groups is situated at lower wavenumbers than the two CH stretching components.

The calculated vibrational transitions, IR, and Raman intensities associated with the ring CH stretches for the calculated structures (given only for ion pair dimers involving B_{Mim}^+ and O_{Mim}^+ cations) are reported in Table 5 (values for calculated ion pair dimers involving other cations can be provided upon request). The vibrational analysis carried out here confirms the previous assignments. The CH stretching modes associated with the $NC_2(H)N$ group are sensitive to the structural organization within the ion pair dimer, and their vibrational transitions overlap a larger range in the CH spectral region (cf., Table 5). In IR absorption spectroscopy, only the CH stretching modes associated with the acidic $C_2(H)$ group of imidazolium rings exhibit a significant intense absorption lines, whereas the stretches associated with HCCH of the imidazolium rings show a significant intensity in Raman spectroscopy.

The influence of water interacting with the ion pair does not lead to drastic spectral modifications of the CH stretches associated with the HCCH groups of the imidazolium rings within ion pair dimers involving either BF_4^- or PF_6^- anions (cf., Table 5). The position and the relative intensity of these modes (symmetric and antisymmetric) do not show noticeable perturbations due to the presence of water. In this context, our calculations agree with the fact that Raman scattering features in this region do not show appreciable changes in the presence of water (band center positions and relative intensities) in this spectral range (3000−3200 cm^{-1}).[42]

In contrast, for the CH mode involving the most acidic proton, the perturbations due to the presence of water are found more noticeable than for the two previous ones. Nevertheless, their band center positions are not situated in a characteristic spectral region and overlap with the two other CH stretches. Because water does not specifically interact with imidazolium cations, these spectral signatures do not result straightforwardly from perturbations induced by water but result from interactions (structural reorganization) within the ion pair dimer.

IV. Discussion and Conclusion

Finally, our theoretical calculations provide some physical insight about the nature of the interaction of water highly diluted in 1-alkyl-3-methyl imidazolium ILs and to interpret qualitatively the local organization of water in ILs in symmetric structures A···H−O−H···A. First, the local organization between the ionic species (ion pair dimer) is preliminary governed by electrostatic interactions. Although the hydrogen-bond formation between the cation and the anions has been sometimes invoked[89−95] (between the F atom of the anions and the acidic $C_{(2)}H$ proton of the imidazolium cations), such $C_{(2)}H$···F hydrogen-bond interactions exhibit a lack of direc-

TABLE 5: Calculated Fundamental Transitions ν_{cal} and IR and Raman Intensities of the Imidazolium Ring Stretching Modes within the Ion Pair Dimers Involving Either PF_6^- or BF_4^- Anions [B3LYP/6-31+G][a]**

ν (cm^{-1})	intensities I_{IR} (km/mol)	I_{Ram} (Å^4/amu)	ν (cm^{-1})	intensities I_{IR} (km/mol)	I_{Ram} (Å^4/amu)	ion pair dimer modes assignment
$H_2O\cdot\{PF_6^-\cdot C_{4Mim}^+\}_2$			$\{PF_6^-\cdot C_{4Mim}^+\}_2$			PF stretches
693.5	7.9	16.1	690.7	10.8	16.8	ν_s(PF) str.
688.6	44.0	14.3	687.6	40.8	11.3	
						ring CH stretches
3316.5	1.4	111.2	3316.6	15.3	65.0	HCCH sym str.
3315.0	0.9	117.0	3315.0	0.3	132.0	
3297.6	6.1	54.0	3298.2	5.1	51.8	HCCH asym. str.
3296.5	5.1	49.8	3296.5	12.2	53.4	
3284.2	121.8	70.0	3326.1	113.7	113.5	$NC_2(H)N$ CH str
3235.0	256.4	63.1	3296.9	181.2	44.2	
$H_2O\cdot\{PF_6^-\cdot C_{8Mim}^+\}_2$			$\{PF_6^-\cdot C_{8Mim}^+\}_2$			PF stretches
691.8	14.2	17.7	690.6			ν_s(PF) str.
687.7	48.8	14.0	688.0			
						ring CH stretches
3316.7	0.1	121.3	3315.6	10.5	18.1	HCCH sym str.
3315.2	1.1	104.9	3314.8	38.2	11.2	
3298.0	10.3	48.6	3297.6	18.1	47.6	HCCH asym. str.
3296.6	5.2	46.4	3296.4	1.1	137.1	
3299.7	175.6	59.9	3323.5	5.2	48.8	$NC_2(H)N$ CH str
3277.9	168.4	66.2	3296.4	5.2	51.1	
$H_2O\cdot\{BF_4^-\cdot C_{4Mim}^+\}_2$			$\{BF_4^-\cdot C_{4Mim}^+\}_2$			BF stretches
746.3	3.3	9.9	746.5	1.0	7.7	ν_s(BF) str.
746.1	43.3	0.1	746.2	11.0	0.5	
						ring CH stretches
3314.9	1.5	115.0	3316.0	2.7	103.9	HCCH sym str.
3314.8	1.7	119.6	3318.8	2.9	104.7	
3296.7	5.0	50.0	3300.7	5.6	43.1	HCCH asym. str.
3296.5	4.9	51.5	3300.3	5.7	43.3	
3249.6	237.7	61.5	3210.1	418.4	48.3	$NC_2(H)N$ CH str
3234.0	212.3	79.6	3203.4	145.0	120.1	
$H_2O\cdot\{BF_4^-\cdot C_{8Mim}^+\}_2$			$\{BF_4^-\cdot C_{8Mim}^+\}_2$			
						BF stretches
746.4	3.6	8.6	746.3	10.1	1.4	ν_s(BF) str.
746.2	41.8	0.2	746.5	1.0	9.1	
						ring CH stretches
3314.9	1.5	109.3	3319.3	2.8	96.0	HCCH sym str.
3314.8	1.7	114.5	3318.9	3.0	98.7	
3296.7	4.9	47.8	3301.0	5.5	39.6	HCCH asym. str.
3296.5	4.7	49.3	3300.2	5.5	40.7	
3250.6	229.2	59.9	3211.7	390.6	54.1	$NC_2(H)N$ CH str
3234.3	209.7	76.6	3203.7	166.8	112.8	

[a] At this computational level (DFT-B3LYP/6-31+G**), the calculated vibrational transitions associated with the symmetric PF and BF stretches of the PF_6^- or BF_4^- anions (Raman active) are 741 and 690 cm^{-1}, respectively.

tionality. A theoretical analysis has shown that such hydrogen bond of imidazolium $C_{(2)}H$ with surrounding BF_4^- or PF_6^- anions is not essential for the attraction and only contributes to the stabilization energy of such cation−anion pairs.[96,105] Clearly, our DFT calculations lead to the same conclusion. Moreover, our analysis in terms of many-body energy interactions shows that cooperative effects occur in the ion pair dimer ("dry" as well as "wet"). The structural organization does not result from a simple superposition of pairwise interactions as expected in ionic systems. Non additive interactions are also involved, and mainly the destabilizing 3-bodies (3-bodies-), even if they contribute to only 10−15% of the total interaction energy (cf., Table 3). This finding markedly underlies the necessity to consider the cation−anion pair dimer in quantum chemistry calculations as the minimal entity representative of the polar network of ILs, especially for investigating the local structure (despite the limitation due to the truncation of the long-range electrostatic forces) and more particularly the vibrational spectra of "monomeric" water in ILs. Finally, the local organization between ions precludes any specific interactions between water and the imidazolium rings (with the acidic proton).

Non additive interactions are also involved in the solvation mechanism of water in ILs and play a determining role by favoring interactions of water with two anions in symmetric A···H−O−H···A structures. From our DFT calculations, the energy interaction of water attached to the polar network (via two anions) is estimated at about −12 kcal/mol (i.e., −6 kcal/mol for one intermolecular bond, cf., Table 3).

The vibrational analysis led to IR and Raman spectral signatures of water (shifts, separation of the OH stretches, as well as the IR and Raman intensity ratios), which are qualitatively in good agreement with the measured IR and Raman profiles (cf., Figure 7). This allows one to legitimize the associations of water doubly hydrogen-bonded with two anions as being representatives of local organization predominantly encountered in real water/ILs mixtures at least at low water concentrations. In such nearly "symmetric" A···H−O−H···A structures, the OH bond lengths of water are found equally perturbed by the interactions with the anions and less affected than for water in asymmetric H-bonded associations (SD water). Thus, the shifts of the ν_1 and ν_3 modes of water in such symmetric associations with anions are found quite comparable

to those found in usual "weak" hydrogen-bonded water in molecular systems (as water/benzene, for instance), while the interaction energy is typically about 3 times more stabilizing.

Our study also provides some insights about the pertinence of other vibrational modes associated with the distinct anion/cation couples with respect to the insertion of a molecular compound such as water (at very low concentration). First, the symmetric XF stretches of the anions (X = P for PF_6^- or X = B for BF_4^-) are found blue-shifted by a few wavenumbers (<5 cm^{-1}) in the presence of water. This finding agrees with recent Raman measurements for water/B_{Mim}/BF_4 mixtures, providing evidence of such a shift of the band associated with the BF stretching mode evolving with the concentration of water.[42] Although the vibrational analysis associated with the CH modes of the imidazolium cations is more delicate due to possible overlap between the two CH stretches of the HCCH groups and the CH stretching mode of the $NC_2(H)N$ groups (acidic proton) as well as their sensitivity to perturbations of their closest environment, our calculations do not show noticeable modifications of the CH stretch involving the acidic proton in the presence of water (comparison between "dry" and "wet" ion pair dimers, Table 5). This finding nicely agrees with the previous conclusion supported by ATR-IR and Raman measurements[42,47] that "monomeric" water does not specifically interact with the acidic proton of the 1-alkyl-3-methyl imidazolium cations.

Finally, we conclude that the vibrational spectra of the OH stretching modes of water dissolved in 1-alkyl-3-methyl imidazolium ILs (3500−3800 cm^{-1}) can be interpreted on the ground of a local organization of monodispersed water forming hydrogen-bonded nearly "symmetric" structures of type A···H−O−H···A (A = either PF_6^- or BF_4^-). The doubly hydrogen-bonded character of water in such associations is mainly characterized by specific spectral features consistent with those observed for water highly diluted in imidazolium ILs mixtures involving PF_6^- or BF_4^- anions. These specific spectral features of water rely upon the shifts of the ν_1 and ν_3 stretching modes of water as well as the separation $\Delta\nu_{13}$ between them (about 80−90 cm^{-1}) and their intensity ratio estimates R (IR absorption and Raman). Nevertheless, the appearance in Raman scattering of a well-defined band of the ν_3 mode of water occurs in our study as a new specific spectral feature of water diluted in 1-alkyl-3-methyl imidazolium. This activity results from a significant intensity enhancement of this mode of water in ILs, which is even not observed in molecular systems involving H-bonded complexes of water. Thus, we emphasize the noticeable electrostatic character of the hydrogen-bond interactions of water with the anions through the significant polarization of water due to the local electrostatic fields induced by ions.

Acknowledgment. We gratefully acknowledge the support provided by the M3PEC computer centre of the DRIMM (Direction des Ressources Informatiques et Multimédia Mutualisée, Talence, France) of the University of Bordeaux I and the IDRIS computer centre of the CNRS (Institut du Développement et des Ressources en Informatique Scientifique, Orsay, France) for allocating computing time and providing facilities. M.B. is also indebted to the GRICE-CNRS PICS program, which provided financial support for his stay in Portugal to discuss results corresponding to part of the current Article.

References and Notes

(1) Bessac, F.; Maseras, F. *J. Comput. Chem.* **2008**, *29*, 892–899.
(2) Tindale, J. J.; Na, C.; Jennings, M. C.; Ragogna, P. J. *Can. J. Chem.* **2007**, *85*, 660–667.
(3) Germani, R.; Mancini, M. V.; Savelli, G.; Spreti, N. *Tetrahedron Lett.* **2007**, *48*, 1767–1769.
(4) Huddleston, J. G.; Willauer, H. D.; Swatloski, R. P.; Visser, A. E.; Rodgers, R. D. *Chem. Commun.* **1998**, 1765–1766.
(5) Keskin, S.; Kayrak, D.; Akman, U.; Hortaçsu, O. *J. Supercrit. Fluids* **2007**, *43*, 150–180.
(6) Brennecke, J. F.; Marginn, E. J. *AIChE J.* **2001**, *47*, 2384–2389.
(7) Chiappe, C.; Pieraccini, D. *J. Phys. Org. Chem.* **2005**, *18*, 275–297.
(8) Endres, F.; Abedin, S. Z. E. *Phys. Chem. Chem. Phys.* **2006**, *8*, 2101–2116.
(9) Marsh, K. N.; Boxall, J. A.; Lichtenthaler, R. *Fluid Phase Equilib.* **2004**, *219*, 93–98.
(10) Wishart, J. F.; Castner, E. W. *J. Phys. Chem. B* **2007**, *111*, 4639.
(11) Daguenet, C.; Dyson, P. J.; Krossing, I.; Oleinikova, A.; Slattery, J.; Wakai, C.; Weingärtner, H. *J. Phys. Chem. B* **2006**, *110*, 12682–12688.
(12) Aki, S. N. V. K.; Brennecke, J. F.; Samanta, A. *Chem. Commun.* **2001**, 413–414.
(13) Wakai, C.; Oleinikova, A.; Ott, M.; Weingärtner, H. *J. Phys. Chem. B* **2005**, *109*, 17028–17030.
(14) Zhang, Z.; Wu, W.; Liu, Z.; HAn, B.; Gao, H.; Jiang, T. *Phys. Chem. Chem. Phys.* **2004**, *6*, 2352–2357.
(15) Najdanavi-Visak, V.; Esperença, J. M. S. S.; Rebel, L. P. N.; Ponte, M. N. d.; Guedes, H. J. R.; Seddon, K. R.; Szydlowski, J. *Phys. Chem. Chem. Phys.* **2002**, *4*, 1701–1703.
(16) Anthony, J. L.; Marginn, E. J.; Brennecke, J. F. *J. Phys. Chem. B* **2001**, *105*, 10942–10949.
(17) Anthony, J. L.; Marginn, E. J.; Brennecke, J. F. *J. Phys. Chem. B* **2002**, *106*, 7315–7320.
(18) Crosthwaite, J. M.; Aki, S. N. V. K.; Marginn, E. J.; Brennecke, J. F. *J. Phys. Chem. B* **2004**, *108*, 5113–5119.
(19) Cadena, C.; Anthony, J. L.; Shah, J. K.; Morrow, T. I.; Brennecke, J. F.; Maginn, E. J. *J. Am. Chem. Soc.* **2004**, *126*, 5300–5308.
(20) Blanchard, L. A.; Gu, Z.; Brennecke, J. F. *J. Phys. Chem. B* **2001**, *105*, 2437–2244.
(21) Lachwa, J.; Bento, I.; Duarte, M. T.; Lopes, J. N. C.; Rebelo, L. P. N. *Chem. Commun.* **2006**, 2445–2447.
(22) Hunt, P. *J. Phys. Chem. B* **2007**, *111*, 4844–4853.
(23) Saha, S.; Hamaguchi, H. *J. Phys. Chem. B* **2006**, *110*, 277–2781.
(24) Mele, A.; Tran, C. D.; Lacerda, S. H. d. P. *Angew. Chem., Int. Ed.* **2003**, *42*, 4364–4366.
(25) Annapureddy, H. V. R.; Hu, Z.; Xia, J.; Margulis, C. J. *J. Phys. Chem. B* **2008**, *112*, 1770–1776.
(26) Seth, D.; Chakraborthy, A.; Setua, P.; Sarkar, N. *J. Chem. Phys.* **2007**, *126*, 224512.
(27) Triolo, A.; Russina, O.; Bleif, H. J.; Cola, E. D. *J. Phys. Chem. B* **2006**, *110*, 4641–4644.
(28) Deschamps, J.; Costa-Gomes, M. F.; Padua, A. A. H. *ChemPhysChem* **2004**, *5*, 1049–1052.
(29) Canongia-Lopes, J.; Deschamps, J.; Padua, A. A. H. *J. Phys. Chem. B* **2004**, *108*, 2038–2047.
(30) Yan, T.; Burnham, C. J.; Popolo, M. G. D.; Voth, G. A. *J. Phys. Chem. B* **2004**, *108*, 11877–11881.
(31) Margulis, C. J.; Stern, H. A.; Berne, B. J. *J. Phys. Chem. B* **2002**, *106*, 12017–12021.
(32) Popolo, M. G. D.; Lynden-Bell, R. M.; Kohanoff, J. *J. Phys. Chem. B* **2005**, *109*, 5895–5902.
(33) Liu, Z.; Huang, S.; Wang, W. *J. Phys. Chem. B* **2004**, *108*, 12978–12989.
(34) Wu, X.; Liu, Z.; Huang, S.; Wang, W. *Phys. Chem. Chem. Phys.* **2005**, *7*, 2771–2779.
(35) Schröder, C.; Wakaï, C.; Weingärtner, H.; Steinhausen, O. *J. Chem. Phys.* **2007**, *126*, 84811.
(36) Yasaka, Y.; Wakai, C.; Matubayasi, N.; Nakahara, M. *J. Phys. Chem. A* **2007**, *111*, 541–543.
(37) Canongia-Lopes, J. N. A.; Padua, A. A. H. *J. Phys. Chem. B* **2006**, *110*, 3330–3335.
(38) Canongia-Lopes, J.; Costa-Gomes, M. F.; Padua, A. H. *J. Phys. Chem. B* **2006**, *110*, 16816–16817.
(39) Jiang, W.; Wang, Y.; Voth, G. A. *J. Phys. Chem. B* **2007**, *111*, 4812–4818.
(40) Wang, Y.; Voth, G. A. *J. Am. Chem. Soc.* **2005**, *127*, 12192–12193.
(41) Dimitrakis, G.; Villar-Garcia, I. J.; Lester, E.; Licence, P.; Kingman, S. *Phys. Chem. Chem. Phys.* **2008**, *10*, 2947–2951.
(42) Fazio, B.; Triolo, A.; Marco, G. D. *J. Raman Spectrosc.* **2007**, *39*, 233–237.
(43) Dominguez-Vidal, A.; Kaun, N.; Ayora-Canada, M. J.; Lendl, B. *J. Phys. Chem. B* **2007**, *111*, 4446–4452.
(44) Lopze-Pastor, M.; Ayora-Canada, M. J.; Valcarcel, M.; Lendl, B. *J. Phys. Chem. B* **2006**, *110*, 10896–10902.
(45) Tran, C. D.; Lacerda, S. H. D. P.; Oliveira, D. *Appl. Spectrosc.* **2003**, *57*, 152–157.

(46) Köddermann, T.; Wertz, C.; Heintz, A.; Ludwig, R. *Angew. Chem., Int. Ed.* **2006**, 3697.
(47) Cammarata, L.; Kazarian, S. G.; Salter, P. A.; Welton, T. *Phys. Chem. Chem. Phys.* **2001**, *3*, 5192–5200.
(48) Besnard, M.; Danten, Y.; Tassaing, T. *J. Chem. Phys.* **2000**, *113*, 3741–3748.
(49) Danten, Y.; Tassaing, T.; Besnard, M. *J. Phys. Chem. A* **2000**, *104*, 9415–9427.
(50) Tassaing, T.; Danten, Y.; Besnard, M. *J. Mol. Liq.* **2002**, *101*, 149.
(51) Tassaing, T.; Danten, Y.; Besnard, M.; Zoidis, E.; Yarwood, J.; Guissani, Y.; Guillot, B. *Mol. Phys.* **1995**, *84*, 769.
(52) Andanson, J. M.; Tassaing, T.; Besnard, M. *J. Chem. Phys.* **2005**, *122*, 174512–174521.
(53) Besnard, M.; Tassaing, T.; Danten, Y.; Andanson, J. M.; Soetens, J. C.; Cansell, F.; Loppinet-Serani, A.; Reveron, H.; Aymonier, C. *J. Mol. Liq.* **2006**, *125*, 88–99.
(54) Oparin, R.; Tassaing, T.; Danten, Y.; Besnard, M. *J. Chem. Phys.* **2004**, *120*, 10691–10698.
(55) Oparin, R.; Tassaing, T.; Danten, Y.; Besnard, M. *J. Chem. Phys.* **2005**, *123*, 224501.
(56) Lalanne, P.; Tassaing, T.; Danten, Y.; Cansell, F.; Tucker, S. C.; Besnard, M. *J. Phys. Chem. A* **2004**, *108*, 2617–2624.
(57) Lalanne, P.; Andanson, J. M.; Soetens, J.-C.; Tassaing, T.; Danten, Y.; Besnard, M. *J. Phys. Chem. A* **2004**, *108*, 3902–3909.
(58) Lalanne, P.; Tassaing, T.; Danten, Y.; Besnard, M. *J. Mol. Liq.* **2002**, *98*−*99*, 201.
(59) Tassaing, T.; Danten, Y.; Besnard, M. *J. Mol. Liq.* **2002**, *98*−*99*, 201.
(60) Backx, P.; Goldman, S. *J. Phys. Chem.* **1981**, *85*, 2975.
(61) Pimentel, G. C.; Clellan, A. L. M. *The Hydrogen Bond*; Reinhold Publishing Corp.: New York, 1960.
(62) *Spectrosocopy and Structure of Molecular Complexes*; Yarwood, J., Ed.; Plenum Press: London and New York, 1973.
(63) Scherer, J. R. In *Advances in Infrared and Raman Spectroscopy*; Clark, R. J. H., Hester, R. E., Eds.; Heyden: 1978; Chapter 3, pp 148−216.
(64) Suzuki, S.; Green, P. G.; Bumgarner, R. E.; Dasgupta, S.; Goddard, W. A.; Blake, G. A. *Science* **1992**, *257*, 942.
(65) Klemperer, W. *Nature* **1993**, *362*, 698.
(66) Engdahl, A.; Nelander, B. *J. Phys. Chem.* **1987**, *91*, 2253–2258.
(67) Engdahl, A.; Nelander, B. *J. Phys. Chem.* **1985**, *89*, 2860–2864.
(68) Augspurger, J. D.; Dykstra, C. E.; Zwier, T. S. *J. Phys. Chem. A* **1992**, *96*, 7252–7257.
(69) Wanna, J.; Menapace, J. A.; Berstein, E. R. *J. Chem. Phys.* **1986**, *85*, 1795–1805.
(70) Kim, K. S.; Lee, J. Y.; Choi, H. S.; Kim, J.; Yang, J. H. *Chem. Phys. Lett.* **1997**, *265*, 497–502.
(71) Bates, J. B. *J. Chem. Phys.* **1971**, *55*, 489.
(72) Quist, A. S.; Bates, J. B.; Boyd, G. E. *J. Chem. Phys.* **1971**, *54*, 4896.
(73) Walrafen, G. E. *J. Chem. Phys.* **1971**, *55*, 768.
(74) Bhargava, B. L.; Balasubramanian, S.; Klein, M. L. *Chem. Commun.* **2008**, 3339–3351.
(75) Shigeto, S.; Hamaguchi, H. *Chem. Phys. Lett.* **2006**, *427*, 329–332.
(76) Santos, L. M. N. B. F.; Lopes, J. N. c.; Coutinho, J. A. P.; Esperança, J. M. S. S.; Gomes, l. R.; Marrucho, I.; Rebelo, L. P. N. *J. Am. Chem. Soc.* **2007**, *129*, 284–285.
(77) Köddermann, T.; Paschek, D.; Ludwig, R. *ChemPhysChem* **2008**, *9*, 549–555.
(78) Frisch, M. J. *Gaussian 03*; Gaussian, Inc.: Wallingford, CT, 2004.
(79) Scott, A. P.; Radom, L. *J. Phys. Chem.* **1996**, *100*, 16502–16513.
(80) Boys, S. F.; Bernardi, F. *Mol. Phys.* **1970**, *19*, 553.
(81) Mierzwicki, K.; Latajka, Z. *Chem. Phys. Lett.* **2003**, *380*, 654–664.
(82) Tury, L.; Dannenberg, J. J. *J. Phys. Chem.* **1993**, *97*, 2488–2490.
(83) Valiron, P.; Mayer, I. *Chem. Phys. Lett.* **1997**, *1997*, 46–55.
(84) White, J. C.; Davidson, E. R. *J. Chem. Phys.* **1990**, *93*, 8029.
(85) Wilson, E. B.; Decius, J. C.; Cross, P. C. *Molecular Vibrations*; McGraw-Hill: New York, 1955.
(86) Sinha, P.; Boesch, S. E.; Gu, C.; Wheeler, R. A. *J. Phys. Chem. A* **2004**, *108*, 9213–9217.
(87) Wong, M. W. *Chem. Phys. Lett.* **1996**, *256*, 391–399.
(88) Irikura, K. K.; III, R. D. J.; Kacker, R. N. *J. Phys. Chem. A* **2005**, *109*, 8430–8437.
(89) Heimer, N. E.; Sesto, R. E. D.; Meng, Z.; Wilkes, J. S.; Carper, W. R. *J. Mol. Liq.* **2006**, *124*, 84–95.
(90) Meng, Z.; Dölle, A.; Carper, W. R. *J. Mol. Struct. (THEOCHEM)* **2002**, *585*, 119–128.
(91) Morrow, T. I.; Maginn, E. J. *J. Phys. Chem. B* **2002**, *106*, 12807–12813.
(92) Katsyuba, S. A.; Dyson, P. J.; Vandyukova, E. E.; Chernova, A. V.; Vidis, A. *Helv. Chim. Acta* **2004**, *87*, 2556–2565.
(93) Talaty, R.; Raja, S.; Storhaug, V. J.; Dölle, A.; Carper, W. R. *J. Phys. Chem. B* **2004**, *108*, 13177–13184.
(94) Berg, R. W.; Deetlefs, M.; Seddon, K. R.; Shim, I.; Thompson, J. M. *J. Phys. Chem. B* **2005**, *109*, 19018–19025.
(95) Umebayashi, Y.; Fujimori, T.; Sukizaki, T.; Asada, M.; Fujii, K.; Kanzaki, R.; Ishiguro, S. *J. Phys. Chem. A* **2005**, *109*, 8976–8982.
(96) Tsuzuki, S.; Tokuda, H.; Hayamizu, K.; Watanabe, M. *J. Phys. Chem. B* **2005**, *109*, 16474–16481.
(97) Wood, J. L. The Vibrational Spectra of Hydrogen Bonded Complexes. In *Spectroscopy and Structure of Molecular Complexes*; Yarwood, J., Ed.; Plenum Press: London and New York, 1973.
(98) Wang, Y.; Li, H.; Han, S. *J. Phys. Chem. B* **2006**, *110*, 24646–24651.
(99) Li, W.; Qi, C.; Wu, X.; Rong, H.; Gong, L. *J. Mol. Struct. (THEOCHEM)* **2008**, *855*, 34–39.
(100) Porter, A. R.; Liem, S. Y.; Popelier, P. L. A. *Phys. Chem. Chem. Phys.* **2088**, *10*, 4240–4248.
(101) Schröder, C.; Rudas, T.; Neumayr, G.; Benkner, S.; Steinhauser, O. *J. Chem. Phys.* **2007**, *127*, 234503.
(102) Moreno, M.; Castiglione, F.; Mele, A.; Pasqui, C.; Raos, G. *J. Phys. Chem. B* **2008**, *112*, 7826–7836.
(103) Bhargava, B. L.; Balasubramanian, S. *J. Phys. Chem. B* **2007**, *111*, 4477–4487.
(104) Köddermann, T.; Wertz, C.; Heintz, A.; Ludwig, R. *ChemPhysChem* **2006**, *7*, 1944–1949.
(105) Tsuzuki, S.; Tokuda, H.; Mikami, M. *Phys. Chem. Chem. Phys.* **2007**, *9*, 4780–4784.

JP8108368